

# QED in Monte Carlo applied to radiative lepton decays

Z. Was\*,

\*Institute of Nuclear Physics, Polish Academy of Sciences, Krakow

(A) `photos` is the Monte Carlo of the after-burner type that is it reads in information from event record, modifies it with added photons (or leptons) and store the events back.

(B) Despite the algorithm is universal that does not mean it has to be of the approximation only.

1. Aim of my talk is to provide some information why algorithm can be of high precision.
2. In particular I would like to provide some information why it can be improved decay channel by decay channel, and also why form-factors can be then installed in the program.
3. Fortran version is documented in *Comput.Phys.Commun.* 79 (1994) 291-308 (some modifications introduced later)
4. C++ version is documented in: *Comput.Phys.Commun.* 199 (2016) 86 (some modifications introduced later in particular about emission of lepton pairs produced through exotic states)

5. Project web pages are at present at: <https://wasm.web.cern.ch/wasm/f77.html>  
<http://photospp.web.cern.ch/photospp/>

(C) I have rewritten my talk, thanks to previous presentations.

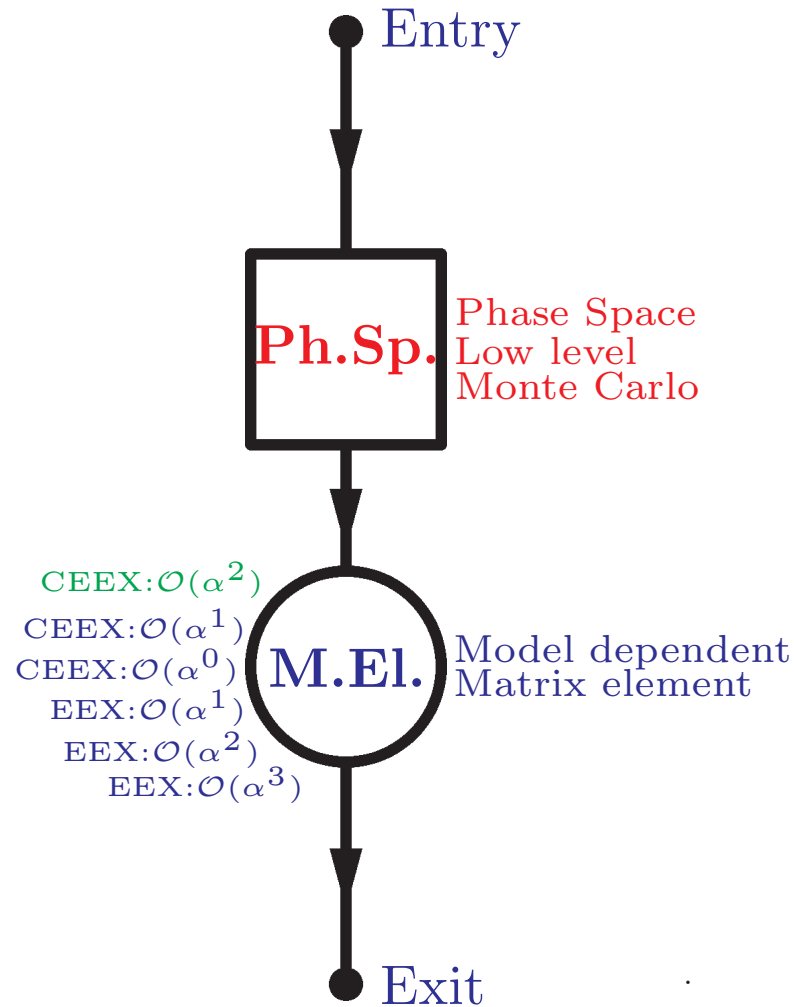
My goal is to provide background for mesons structure dependent form-factors introduction.

**I am not too comfortable with the outcome...**

My first steps for `photos` were on paths from Luminy toward Calanques, some time in  
~ 1985.

**At that time I was not comfortable with the outcome too ...**

## KKMC or PHOTOS rigorous “matrix element $\times$ full phase space” implementation



- Phase-space Monte Carlo simulator is a module producing “raw events” (including importance sampling for possible intermediate resonances/singularities)
- Library of Matrix Elements; input for “model weight”; independent module
- KKMC for  $e^+e^- \rightarrow \tau^+\tau^-n\gamma$  and PHOTOS for radiative corrections in decays are non-Markovian algorithms, photons are generated independently first, phase space constraints are added later, thanks to conformal symmetry of eikonal QED part KKMC or iteratively, Kinoshita-Lee-Nauenberg theorem, for PHOTOS.
- KKMC handle initial state radiation, PHOTOS massive states emission too.

$$Lips_{n+1} \rightarrow Lips_n$$

Orthodox Lorentz-invariant phase space (*Lips*) is in use in PHOTOS!

$$\begin{aligned} dLips_{n+1}(P) &= \\ & \frac{d^3 k_1}{2k_1^0 (2\pi)^3} \cdots \frac{d^3 k_n}{2k_n^0 (2\pi)^3} \frac{d^3 q}{2q^0 (2\pi)^3} (2\pi)^4 \delta^4 \left( P - \sum_1^n k_i - q \right) \\ &= d^4 p \delta^4 (P - p - q) \frac{d^3 q}{2q^0 (2\pi)^3} \frac{d^3 k_1}{2k_1^0 (2\pi)^3} \cdots \frac{d^3 k_n}{2k_n^0 (2\pi)^3} (2\pi)^4 \delta^4 \left( p - \sum_1^n k_i \right) \\ &= d^4 p \delta^4 (P - p - q) \frac{d^3 q}{2q^0 (2\pi)^3} dLips_n(p \rightarrow k_1 \dots k_n). \end{aligned}$$

Introduce factor equal 1:  $d^4 p$  of four-vector  $p$ , times  $\delta^4(p - \sum_1^n k_i)$ , and another factor equal 1, integration variable  $dM_1$  times  $\delta(p^2 - M_1^2)$ .

## *Phase Space Formula of Photos*

$$dLips_{n+1}(P \rightarrow k_1 \dots k_n, k_{n+1}) = dLips_n^{+1 \text{ tangent}} \times W_n^{n+1},$$

$$dLips_n^{+1 \text{ tangent}} = dk_\gamma d\cos\theta d\phi \times dLips_n(P \rightarrow \bar{k}_1 \dots \bar{k}_n),$$

$$\{k_1, \dots, k_{n+1}\} = \mathbf{T}(k_\gamma, \theta, \phi, \{\bar{k}_1, \dots, \bar{k}_n\}). \quad (1)$$

1. If  $dLips_n(P)$  was exact, then this formula is exact parametrization of  $dLips_{n+1}(P)$
2. Practical implementation: Take the configurations from n-body phase space.
3. Turn it back into some coordinate variables.
4. construct new kinematical configuration from all variables.
5. **Forget about temporary  $k_\gamma \theta \phi$ . Only weight  $W_n^{n+1}$  and four vectors count.**
6. Simultaneous use of several  $\mathbf{T}$  is possible and necessary/convenient if more than one charge is present in final state.
7. Choice for  $\mathbf{T}$  construction depend on matrix element: must tangent at singularities, see next slide.

## *Phase Space: (main formula)*

If we choose

$$G_n : M_{2\dots n}^2, \theta_1, \phi_1, M_{3\dots n}^2, \theta_2, \phi_2, \dots, \theta_{n-1}, \phi_{n-1} \rightarrow \bar{k}_1 \dots \bar{k}_n \quad (2)$$

and

$$G_{n+1} : k_\gamma, \theta, \phi, M_{2\dots n}^2, \theta_1, \phi_1, M_{3\dots n}^2, \theta_2, \phi_2, \dots, \theta_{n-1}, \phi_{n-1} \rightarrow k_1 \dots k_n, k_{n+1} \quad (3)$$

then

$$\mathbf{T} = G_{n+1}(k_\gamma, \theta, \phi, G_n^{-1}(\bar{k}_1, \dots, \bar{k}_n)). \quad (4)$$

The ratio of the Jacobians form the phase space weight  $W_n^{n+1}$  for the transformation. Such solution is universal and valid for any choice of  $G$ 's. However,  $G_{n+1}$  and  $G_n$  has to match matrix element, otherwise algorithm will be inefficient (factor  $10^{10}$  ...).

In case of PHOTOS  $G_n$ 's

$$W_n^{n+1} = k_\gamma \frac{1}{2(2\pi)^3} \times \frac{\lambda^{1/2}(1, m_1^2/M_{1\dots n}^2, M_{2\dots n}^2/M_{1\dots n}^2)}{\lambda^{1/2}(1, m_1^2/M^2, M_{2\dots n}^2/M^2)}, \quad (5)$$

*Phase Space: (multiply iterated)*

By iteration, we can generalize formula (1) and add  $l$  particles:

$$\begin{aligned}
 dLips_{n+l}(P \rightarrow k_1 \dots k_n, k_{n+1} \dots k_{n+l}) &= \frac{1}{l!} \prod_{i=1}^l \left[ dk_{\gamma_i} d \cos \theta_{\gamma_i} d\phi_{\gamma_i} W_{n+i-1}^{n+i} \right] \\
 &\times dLips_n(P \rightarrow \bar{k}_1 \dots \bar{k}_n), \\
 \{k_1, \dots, k_{n+l}\} &= \mathbf{T}(k_{\gamma_l}, \theta_{\gamma_l}, \phi_{\gamma_l}, \mathbf{T}(\dots, \mathbf{T}(k_{\gamma_1}, \theta_{\gamma_1}, \phi_{\gamma_1}, \{\bar{k}_1, \dots, \bar{k}_n\}) \dots).
 \end{aligned} \tag{6}$$

Note that variables  $k_{\gamma_m}, \theta_{\gamma_m}, \phi_{\gamma_m}$  are used at a time of the  $m$ -th step of iteration only, and are not needed elsewhere in construction of the physical phase space; the same is true for invariants and angles  $M_{2\dots n}^2, \theta_1, \phi_1, \dots, \theta_{n-1}, \phi_{n-1} \rightarrow \bar{k}_1 \dots \bar{k}_n$  of (2,3), which are also redefined at each step of the iteration. Also intermediate steps require explicit construction of temporary  $\bar{k}'_1 \dots \bar{k}'_n \dots \bar{k}'_{n+m}$ , statistical factor  $\frac{1}{l!}$  added.

We have got **exact distribution of weighted** events over  $n + l$  body phase space.

## *Phase Space Formula: multichannels.*

Often MC algorithm has to be split into branches. In the most general case, when  $n$  different parametrisations of the phase space with different orderings of particles are in use, the cross section can be written as follows:

$$d\Gamma_X = \sum_{\lambda=1}^n \int_0^1 \prod_{i=1}^m dx_i P_\lambda \left[ \sum_{\delta=1}^n P_\delta J_\delta^{-1}(q_1(\lambda, x_i), \dots, q_k(\lambda, x_i)) \right]^{-1} \times |M|^2.$$

In the above formula the four-momenta  $q_i(\lambda, x_i)$  are calculated from the random numbers  $x_i$  according to the parametrization of the phase space of type  $\lambda$ . The Jacobians  $J_\delta$  have to be calculated for all parametrisations of the phase space at the point  $q_i$ ;  $P_\lambda$  denotes the probability of choosing the parametrization of type  $\lambda$  in the generation,  $\lambda$  thus takes<sup>a</sup> a role of an additional discrete variable in the generation. Numerical values of probabilities  $P_\lambda$  do not affect the final distributions, but only the efficiency of the generation.

---

<sup>a</sup>But not  $\delta$ .



## *Phase Space case of complex singularity structure*

- Several  $G_{n+1}$  can be used simultaneously (branching of the generation algorithm).
- Each  $G_{n+1}$  can be used presample distinct singularities.
- The price:  $W_n^{n+1}$  is more complicated but all remain exact.
- **HOWEVER:** We have observed that while matching Jacobians for the two branches related to collinear singularity of photons along direction of  $l^+$  and  $l^+$  (in  $Z$  decay) approximation must be used if more than one photon is present in final state. Otherwise solution become inconsistent. Phase space is not iterative, whereas matrix element for multi-photon state is obtained by iteration.
- **AVOID INCONSISTENCY:** in expanding manifold curvature: must be the same for phase space and Matrix Element. Phase space is manifold, Matrix element squared – bi-linear form on it. Truncation of perturbative expansion or iterative solutions mean truncation in powers of Ricci tensor, this has to be consistent. **Multi-channel phase space is not iterative, single branch algorithm we explained before is that is OK for expansion and exact phase space remain. I have learned that hard way.**

*Phase Space: (multiply iterated)*

We have generalized formula phase space formula to case of  $l$  particles added:

$$\begin{aligned}
 dLips_{n+l}(P \rightarrow k_1 \dots k_n, k_{n+1} \dots k_{n+l}) &= \frac{1}{l!} \prod_{i=1}^l \left[ dk_{\gamma_i} d \cos \theta_{\gamma_i} d\phi_{\gamma_i} W_{n+i-1}^{n+i} \right] \\
 &\times dLips_n(P \rightarrow \bar{k}_1 \dots \bar{k}_n), \tag{7} \\
 \{k_1, \dots, k_{n+l}\} &= \mathbf{T}(k_{\gamma_l}, \theta_{\gamma_l}, \phi_{\gamma_l}, \mathbf{T}(\dots, \mathbf{T}(k_{\gamma_1}, \theta_{\gamma_1}, \phi_{\gamma_1}, \{\bar{k}_1, \dots, \bar{k}_n\}) \dots).
 \end{aligned}$$

*Now we have to start talking about matrix elements:* Our relation between  $n$  and  $n+l$  body phase space is motivated by cancellation of infrared singularities. It provides kind of **triangulation**. Measure defining distance between points from manifolds of distinct no. of particles. Such phase space points are close if they differ by presence of soft photons only.

Experimental user attention necessary. Can 1 GeV photon be ignored or only 0.1 MeV one.

We will move now from **exact distribution** of **weighted** events over  $n + l$  body phase space to case where  $l$  is parameter too, but all remain exact!

## Crude Distribution and crude matrix element

If we add **arbitrary** factors  $f(k_{\gamma_i}, \theta_{\gamma_i}, \phi_{\gamma_i})$  and sum over  $l$  we obtain:

$$\sum_{l=0} \exp(-F) \frac{1}{l!} \prod_{i=1}^l f(k_{\gamma_i}, \theta_{\gamma_i}, \phi_{\gamma_i}) dLips_{n+l}(P \rightarrow k_1 \dots k_n, k_{n+1} \dots k_{n+l}) =$$

$$\sum_{l=0} \exp(-F) \frac{1}{l!} \prod_{i=1}^l \left[ f(k_{\gamma_i}, \theta_{\gamma_i}, \phi_{\gamma_i}) dk_{\gamma_i} d \cos \theta_{\gamma_i} d\phi_{\gamma_i} W_{n+i-1}^{n+i} \right] \times$$

$$dLips_n(P \rightarrow \bar{k}_1 \dots \bar{k}_n), \tag{8}$$

$$\{k_1, \dots, k_{n+l}\} = \mathbf{T}(k_{\gamma_l}, \theta_{\gamma_l}, \phi_{\gamma_l}, \mathbf{T}(\dots, \mathbf{T}(k_{\gamma_1}, \theta_{\gamma_1}, \phi_{\gamma_1}, \{\bar{k}_1, \dots, \bar{k}_n\}) \dots),$$

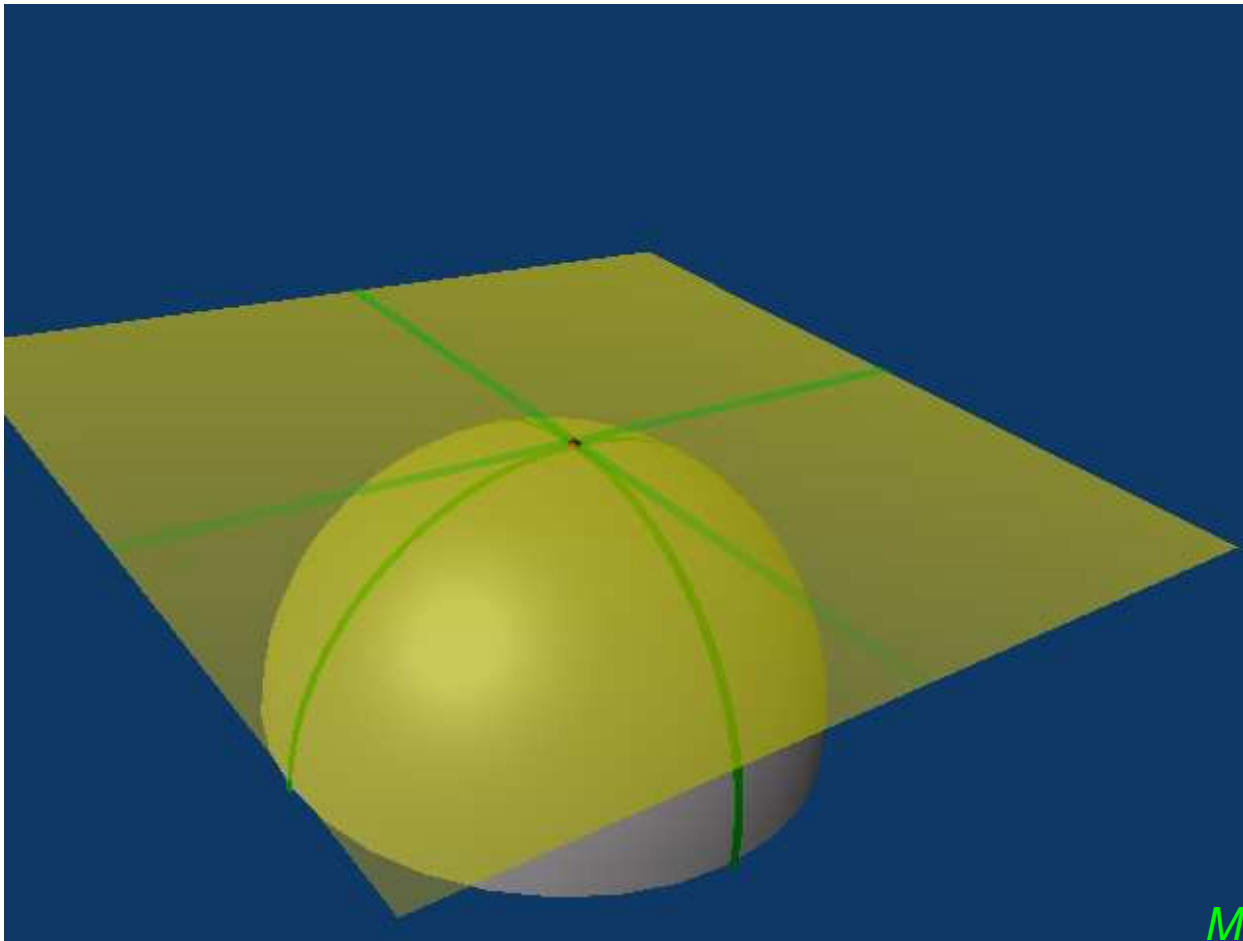
$$F = \int_{k_{min}}^{k_{max}} dk_{\gamma} d \cos \theta_{\gamma} d\phi_{\gamma} f(k_{\gamma}, \theta_{\gamma}, \phi_{\gamma}). \leftarrow \text{KLN good start}$$

- The **olive** parts of rhs. give crude distribution over tangent space, orthogonal  $(k_i, \theta_i, \phi_i)$ .  
We restrict phase space by  $k_{min}$  (typically  $10^{-6}$ )  $k_{max}$  arbitrary (boundary by  $W_{n+i-1}^{n+i}$ ).

## *Heuristic CW complexes*

We define our crude distribution over yellow space (surface=1) (represented by sum of: red point, green lines and flat yellow square). Later we do projections into physics space, using  $\mathbf{T}$  and matrix elements.

*NOTE: in KKMC YFS exclusive exponentiation – conformal symmetry is used instead.*



There is nothing wrong in the following:

1. When top to the bottom stand alone generators are used, events are constructed from coordinates.
2. However, there is nothing wrong in using homeomorfizm from one manifold to another one; exploit corresponding induced measure too.
3. This of course, only when measure on original manifold is well known !
4. That means original non-bremsstrahlung events must be generated following matrix element  $\times$  phase space paradigm.
5. If not, difficult to control approximations will appear.
6. On the other hand, it does not matter what was the parametrization used in original generator.
7. Precision is not compromised by that.
8. Note that the integrated corner of phase space is of extremely soft photons  $k_{min} \sim 10^{-6,-7}$  where photons formation time is larger that hard process time and classical QED limit is imminent.

## In the last two years:

1. PHOTOS generation was enriched with emissions of extra pairs generated from exotic intermediate states such as dark photons or scalars.
2. That is for your information
3. But is of no importance for applications of interest today.
4. I should recall the message, that algorithm can be downgraded (by initialization switch) to single emissions mode,  $k_{min}$  must be then larger.
5. Such mode is useful in development and installation tests of:  
decay channel dependent, matrix element based, emission kernels.

## Technicalities

- (1) The C++ implementation does not require complicated transfer of event information through consecutive CPU time consuming calls on constructors and destructors of HepMC format event record (several time for each event) that should and can be avoided.
- (2) In PHOTOS the library of decay channel dependent matrix element based kernels is encapsulated
- (3) These kernels are calculated often with the help of scalar QED, which is not fundamental theory. Explicit form of ME is coded and is waiting for form-factors.
- (4) They are coded explicitly so form factors can be added.
- (5) But the user prepared ones can not be passed through pointers, I have bad experiences on that in case of `tauola`. I have prepared, nobody was using.
- **WARNING: off shell matrix elements can not be used directly, they need to have form suitable for multi-photon emissions.** Be careful with Kleiss-Stirling spin amplitude methods

- One of the necessary steps was to verify, that once PHOTOS activated, the lepton spectra will be reproduced as far as the LL corrections to required order.
- Formal solution of QED evolution equation can be written as:

$$D(x, \beta_{ch}) = \delta(1-x) + \beta_{ch} P(x) + \frac{1}{2!} \beta_{ch}^2 \{P \times P\}(x) + \frac{1}{3!} \beta_{ch}^3 \{P \times P \times P\}(x) + \dots \quad (9)$$

where  $P(x) = \delta(1-x)(\ln \varepsilon + 3/4) + \Theta(1-x-\varepsilon) \frac{1}{x} (1+x^2)/(1-x)$   
 and  $\{P \times P\}(x) = \int_0^1 dx_1 \int_0^1 dx_2 \delta(x - x_1 x_2) P(x_1) P(x_2)$ .

- In the LL contributing regions, phase space Jacobian's of PHOTOS trivialize (CPC 1994). The solution above is reproduced by PHOTOS in a straightforward manner, for each of the outgoing charged lines.
- But it is only a limit! **PHOTOS treat phase space exactly and covers all corners.**
- In a similar way (simplifying phase space Jacobians and dropping parts of ME) one can get convinced that distribution of soft photons is as should be for exclusive exponentiation.



- So far we were discussing building blocks, but how does it work in practice?
- Avalanche of numerical results...
- **Important:** We could see that kernel simplified with respect to ME is sufficient for sub-permille precision. → Much easier to use.
- MC-TESTER by P. Golonka, N. Davidson, T. Przedzinski, Z. Was is used for tests. Idea is to generate histograms of all possible invariant masses which can be constructed from final state momenta.
- One can select events, for example only photons of energy above 1 GeV will be considered as final state.
- On one frame distribution from two program is printed (in logarithmic scale) and their ration (in linear scale).
- No of events of distinct (in the selected way) final states is printed too.

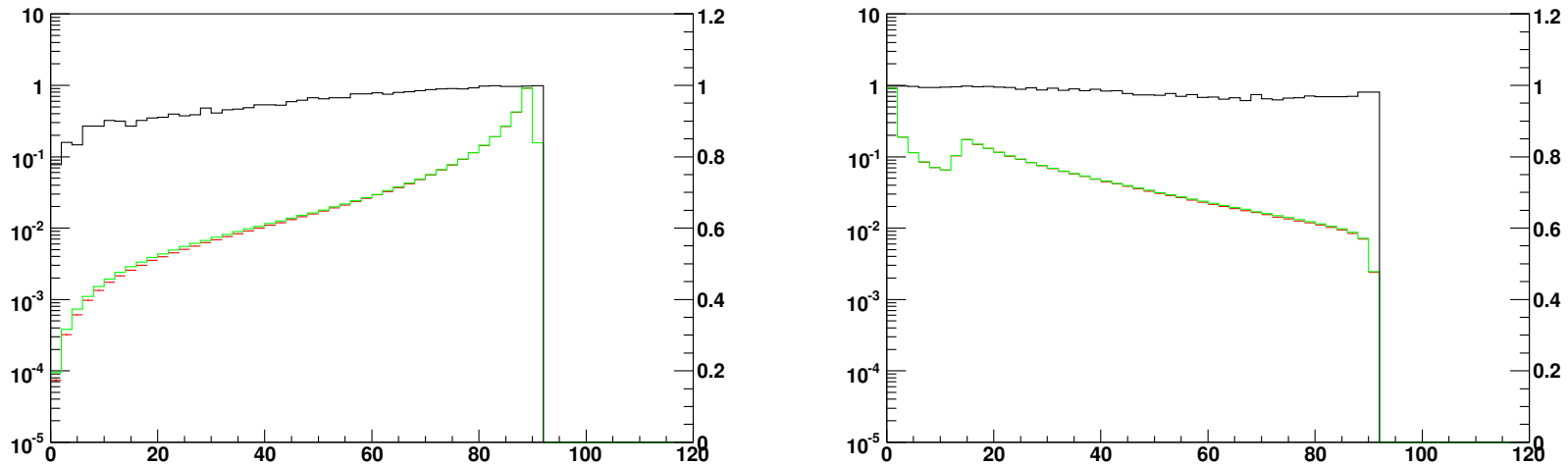


Figure 1: Comparison of standard PHOTOS and KORALZ for single photon emission. In the left frame the invariant mass of the  $\mu^+ \mu^-$  pair;  $SDP=0.00534$ . In the right frame the invariant mass of  $\mu^- \gamma$ ;  $SDP=0.00296$ . The histograms produced by the two programs (logarithmic scale) and their ratio (linear scale, black line) are plotted in both frames. The fraction of events with hard photon was  $17.4863 \pm 0.0042\%$  for KORALZ and  $17.6378 \pm 0.0042\%$  for PHOTOS.

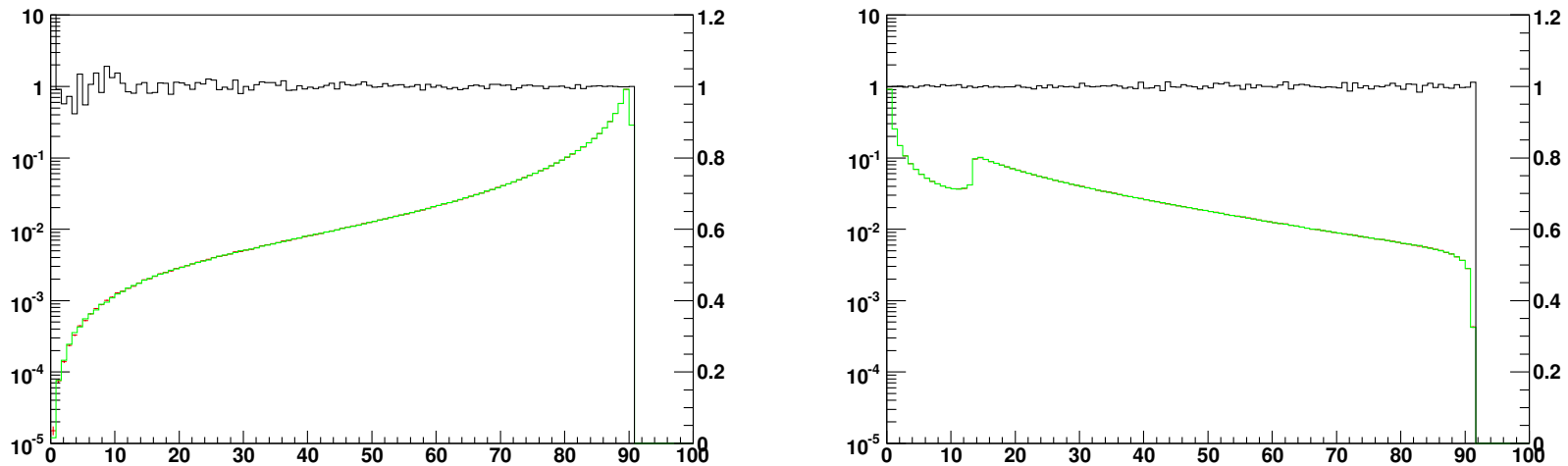


Figure 2: Comparisons of improved PHOTOS and KORALZ for single photon emission. In the left frame the invariant mass of the  $\mu^+ \mu^-$  pair. In the right frame the invariant mass of  $\mu^- \gamma$  pair is shown. In both cases differences between PHOTOS and KORALZ are below statistical error. The fraction of events with hard photon was  $17.4890 \pm 0.0042\%$  for KORALZ and  $17.4926 \pm 0.0042\%$  for PHOTOS.

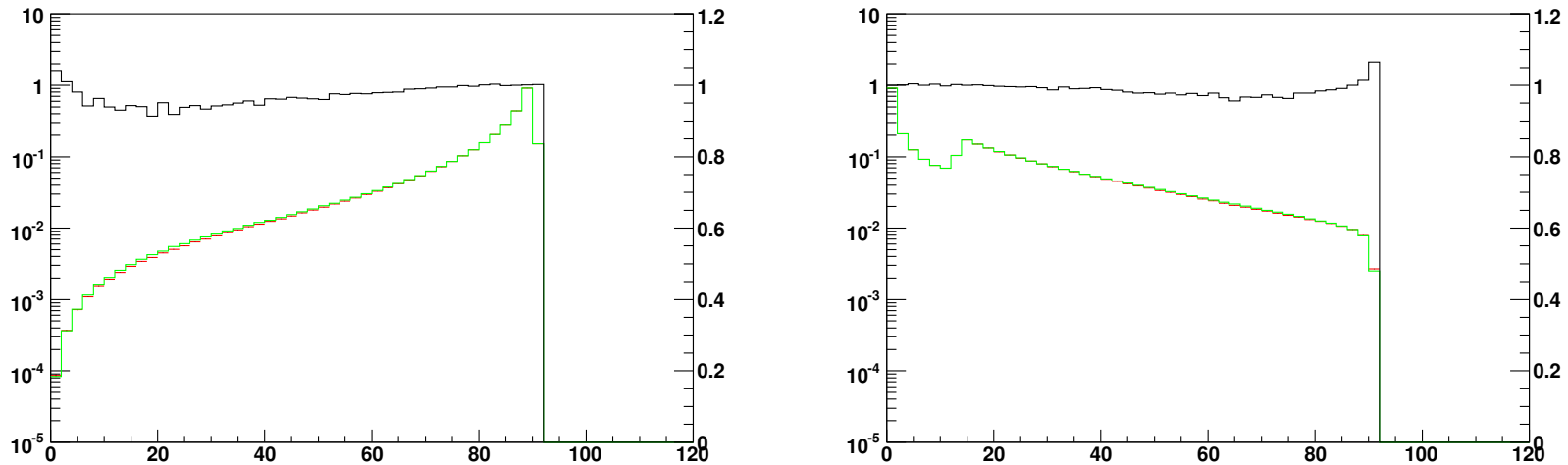


Figure 3: Comparison of standard PHOTOS with multiple photon emission and KKMC with second order matrix element and exponentiation. In the left frame the invariant mass of the  $\mu^+ \mu^-$  pair;  $SDP=0.00409$ . In right frame the invariant mass of the  $\mu^- \gamma$  pair;  $SDP=0.0025$ . The pattern of differences between PHOTOS and KKMC is similar to the one of Fig 1. The fraction of events with hard photon was  $16.0824 \pm 0.0040\%$  for KKMC and  $16.1628 \pm 0.0040\%$  for PHOTOS.

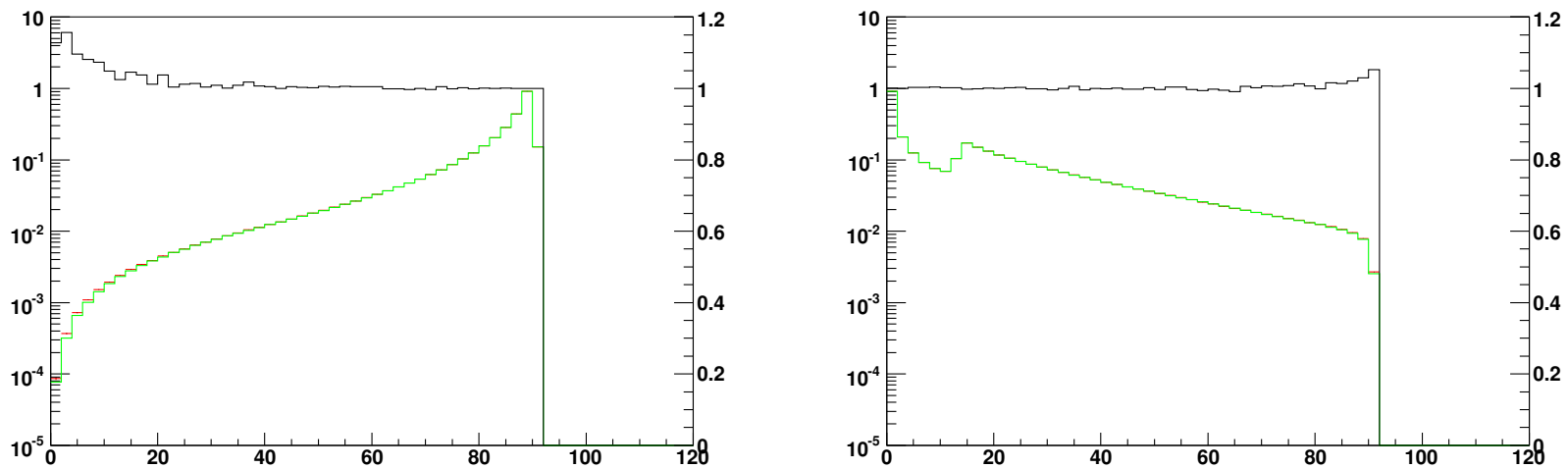


Figure 4: Comparisons of improved PHOTOS with multiple photon emission and KKMC with second order matrix element and exponentiation. In the left frame the invariant mass of the  $\mu^+ \mu^-$  pair;  $SDP=0.0000249$ . In the right frame the invariant mass of the  $\mu^- \gamma$  pair;  $SDP=0.0000203$ . The fraction of events with hard photon was  $16.0824 \pm 0.004\%$  for KKMC and  $16.0688 \pm 0.004\%$  for PHOTOS.

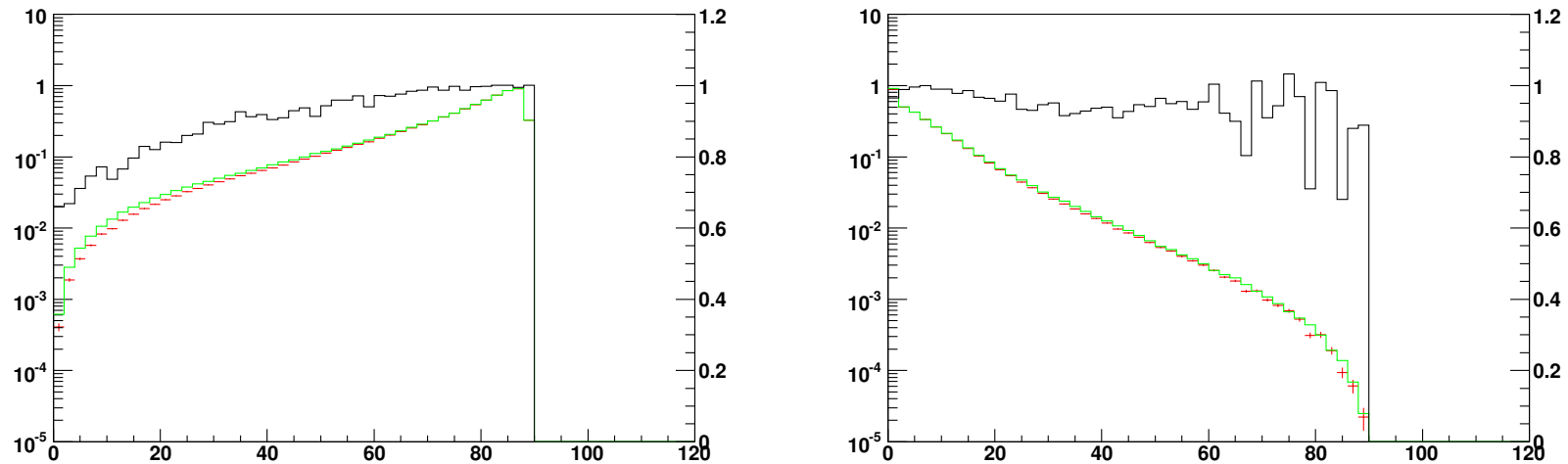


Figure 5: Comparisons of standard PHOTOS with multiple photon emission and KKMC with second order matrix element and exponentiation. In the left frame the invariant mass of the  $\mu^+ \mu^-$  pair;  $SDP= 0.00918$ . In the right frame the invariant mass of the  $\gamma\gamma$  pair;  $SDP=0.00268$ . The fraction of events with two hard photons was  $1.2659 \pm 0.0011\%$  for KKMC and  $1.2952 \pm 0.0011\%$  for PHOTOS.

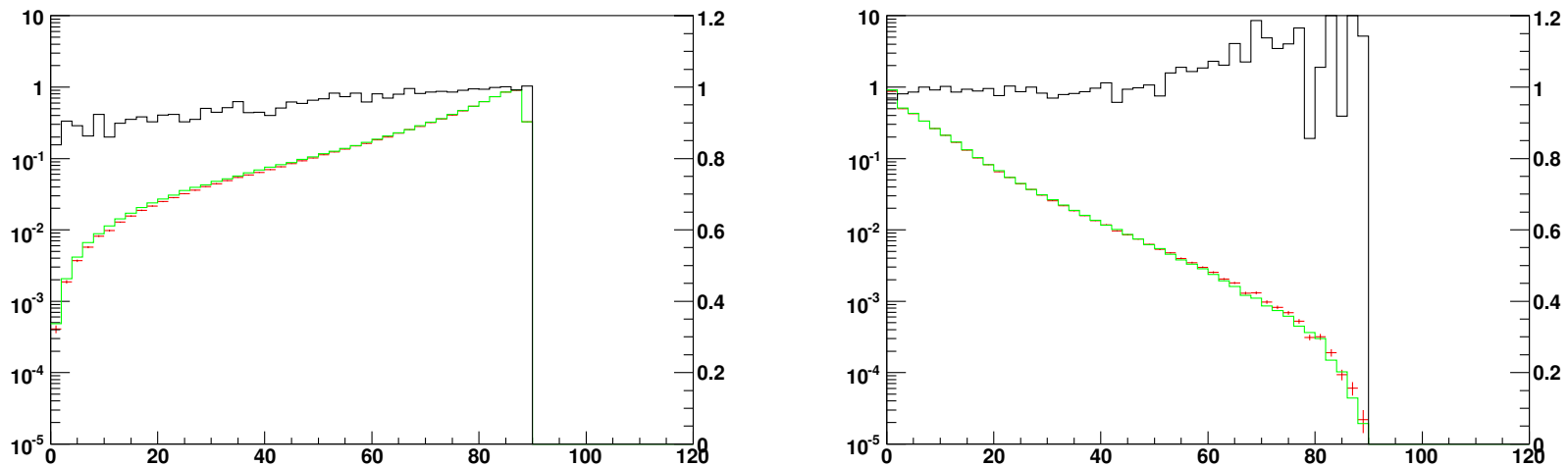


Figure 6: Comparisons of improved PHOTOS with multiple photon emission and KKMC with second order matrix element and exponentiation. In the left frame the invariant mass of the  $\mu^+ \mu^-$  pair;  $SDP= 0.00142$ . In the right frame the invariant mass of the  $\gamma\gamma$ ;  $SDP=0.00293$ . The fraction of events with two hard photons was  $1.2659 \pm 0.0011\%$  for KKMC and  $1.2868 \pm 0.0011\%$  for PHOTOS.

### Matrix Element for $Z$ decay:

- Our discussion of double emission amplitudes was started from the single photon one
- The same is true for amplitudes of other processes. We have to check if they are similar to this for  $Z$  decay.
- In particular only if they structure match we can expect that our discussion of multi-emission may apply as well.

$$I = I^A + I^B + I^C$$

$$I = \mathcal{J} \left[ \left( \frac{p \cdot e_1}{p \cdot k_1} - \frac{q \cdot e_1}{q \cdot k_1} \right) \right] - \left[ \frac{1}{2} \frac{\not{\epsilon}_1 \not{k}_1}{p \cdot k_1} \right] \mathcal{J} + \mathcal{J} \left[ \frac{1}{2} \frac{\not{\epsilon}_1 \not{k}_1}{q \cdot k_1} \right]$$

three gauge invariant parts,  $I^A$  is eikonal;  $I^B, I^C$  carry collinear contrib from  $p$  and  $q$



## Scalar QED: $B \rightarrow K\pi$ decays – pure $I^A$

- The one-loop QED correction to the decay width can be represented as the sum of the Born contribution with the contributions due to virtual loop diagrams and soft and hard photon emissions.

$$d\Gamma^{\text{Total}} = d\Gamma^{\text{Born}} \left\{ 1 + \frac{\alpha}{\pi} \left[ \delta^{\text{Soft}}(m_\gamma, \omega) + \delta^{\text{Virt}}(m_\gamma, \mu_{UV}) \right] \right\} + d\Gamma^{\text{Hard}}(\omega)$$

- where for **Neutral meson decay channels**, hard photon contribution:

$$d\Gamma^{\text{Hard}} = |A^{\text{Born}}|^2 4\pi\alpha \left( q_1 \frac{k_1 \cdot \epsilon}{k_1 \cdot k_\gamma} - q_2 \frac{k_2 \cdot \epsilon}{k_2 \cdot k_\gamma} \right)^2 dLips_3(P \rightarrow k_1, k_2, k_\gamma)$$

- for **Charged meson decay channels**, hard photon contribution:

$$d\Gamma^{\text{Hard}} = |A^{\text{Born}}|^2 4\pi\alpha \left( q_1 \frac{k_1 \cdot \epsilon}{k_1 \cdot k_\gamma} - q \frac{P \cdot \epsilon}{P \cdot k_\gamma} \right)^2 dLips_3(P \rightarrow k_1, k_2, k_\gamma)$$

## Scalar QED for $\gamma^* \rightarrow \pi^+ \pi^- \gamma$ : $I^A$ and non-leading

- This case is different, because of spin structure. One can not make spin of initial state out of internal spin of outgoing particles.

$$H^\mu = \frac{e^2 F_{2\pi}(p^2)}{p^2} \left\{ (q_1 + k - q_2)^\mu \frac{q_1 \cdot \epsilon^*}{q_1 \cdot k} + (q_2 + k - q_1)^\mu \frac{q_2 \cdot \epsilon^*}{q_2 \cdot k} - 2\epsilon^{*\mu} \right\}$$

- As in case of  $Z$  decay one can separate spin amplitude into gauge invariant parts ( $C = \frac{e^2 F_{2\pi}(p^2)}{p^2}$ ):

$$H_I^\mu = C (q_1 - q_2)^\mu \left( \frac{q_1 \cdot \epsilon^*}{q_1 \cdot k} - \frac{q_2 \cdot \epsilon^*}{q_2 \cdot k} \right), H_{II}^\mu = C \left( k^\mu \left( \frac{q_1 \cdot \epsilon^*}{q_1 \cdot k} + \frac{q_2 \cdot \epsilon^*}{q_2 \cdot k} \right) - 2\epsilon^{*\mu} \right), \quad (10)$$

- This can be improved with the following change:

$$H_{I'}^\mu = C \left( (q_1 - q_2)^\mu + k^\mu \frac{q_2 \cdot k - q_1 \cdot k}{q_2 \cdot k + q_1 \cdot k} \right) \left( \frac{q_1 \cdot \epsilon^*}{q_1 \cdot k} - \frac{q_2 \cdot \epsilon^*}{q_2 \cdot k} \right), \quad (11)$$

$$H_{II'}^\mu = C \left( \frac{k^\mu}{q_2 \cdot k + q_1 \cdot k} (q_1 \cdot \epsilon^* + q_2 \cdot \epsilon^*) - \epsilon^{*\mu} \right). \quad (12)$$

- In the second case non-eikonal term is free of collinear logarithm, but is non trivial and contributes 0.2 % to total rate, thus can be numerically studied!

*QED for  $W \rightarrow l\nu_l\gamma$ :  $I^A$ ,  $I^B$  and non-leading*

$$\begin{aligned}
M_{\lambda, \lambda_\nu, \lambda_l}^\sigma(k, Q, p_\nu, p_l) &= \left[ \frac{Q_l}{2k \cdot p_l} b_\sigma(k, p_l) - \frac{Q_W}{2k \cdot Q} (b_\sigma(k, p_l) + b_\sigma(k, p_\nu)) \right] B_{\lambda_l, \lambda_\nu}^\lambda(p_l, Q, p_\nu) \\
&+ \frac{Q_l}{2k \cdot p_l} \sum_{\rho=\pm} U_{\lambda_l, \rho}^\sigma(p_l, m_l, k, 0, k, 0) B_{\rho, -\lambda_\nu}^\lambda(k, Q, p_\nu) \\
&- \frac{Q_W}{2k \cdot Q} \sum_{\rho=\pm} \left( B_{\lambda_l, -\rho}^\lambda(p_l, Q, k) U_{-\rho, -\lambda_\nu}^\sigma(k, 0, k, 0, p_\nu, 0) \right. \\
&\quad \left. + U_{\lambda_l, \rho}^\sigma(p_l, m_l, k, 0, k, 0) B_{\rho, -\lambda_\nu}^\lambda(k, Q, p_\nu) \right), \tag{13}
\end{aligned}$$

$$\begin{aligned}
B_{\lambda_1, \lambda_2}^\lambda(p_1, Q, p_2) &\equiv \frac{g}{2\sqrt{2}} \bar{u}(p_1, \lambda_1) \hat{\epsilon}_W^\lambda(Q) (1 + \gamma_5) v(p_2, \lambda_2), \\
U_{\lambda_1, \lambda_2}^\sigma(p_1, m_1, k, 0, p_2, m_2) &\equiv \bar{u}(p_1, \lambda_1) \hat{\epsilon}_\gamma^\sigma(k) u(p_2, \lambda_2), \\
\delta_{\lambda_1 \lambda_2} b_\sigma(k, p) &\equiv U_{\lambda_1, \lambda_2}^\sigma(p, m, k, 0, p, m), \tag{14}
\end{aligned}$$

$Q_l$  and  $Q_W$  are the electric charges of the fermion  $l$  and the  $W$  boson, respectively, in units of the positron charge,  $\epsilon_\gamma^\sigma(k)$  and  $\epsilon_W^\lambda(Q)$  denote respectively the polarization vectors of the photon and the  $W$  boson. An expression of the function  $U_{\lambda_1, \lambda_2}^\sigma$  in terms of the massless spinors.

*Matrix Element (anything useful seen?):*

- We have seen that in all cases terms  $I^A$ ,  $I^B$ ,  $I^C$  appear
- These are the only ones which carry soft or collinear contributions
- That is why universal weight of Photos could be defined.
- That is also why the solution defined from  $Z$  amplitudes work for other processes as well
- part of reliability proof. Note that it is for spin amplitudes level, thus such corrections do not necessarily break spin correlations. → extra slides
- Tests confirm that ME complete kernel (process dependent) is not necessary even for sub-permille precision level → good for users.

**Nearly complete formula now** if we identify factors  $f(k_{\gamma_i}, \theta_{\gamma_i}, \phi_{\gamma_i})$  with  $I^A$ -s of previous slides. **Still questions of ME not explained** see following slides ...

$$\sum_{l=0} \exp(-F) \frac{1}{l!} \prod_{i=1}^l f(k_{\gamma_i}, \theta_{\gamma_i}, \phi_{\gamma_i}) dLips_{n+l}(P \rightarrow k_1 \dots k_n, k_{n+1} \dots k_{n+l}) =$$

$$\sum_{l=0} \exp(-F) \frac{1}{l!} \prod_{i=1}^l \left[ f(k_{\gamma_i}, \theta_{\gamma_i}, \phi_{\gamma_i}) dk_{\gamma_i} d \cos \theta_{\gamma_i} d\phi_{\gamma_i} W_{n+i-1}^{n+i} \right] \times$$

$$dLips_n(P \rightarrow \bar{k}_1 \dots \bar{k}_n) |M_B(P \rightarrow \bar{k}_1 \dots \bar{k}_n)|^2, \quad (15)$$

$$\{k_1, \dots, k_{n+l}\} = \mathbf{T}(k_{\gamma_l}, \theta_{\gamma_l}, \phi_{\gamma_l}, \mathbf{T}(\dots, \mathbf{T}(k_{\gamma_1}, \theta_{\gamma_1}, \phi_{\gamma_1}, \{\bar{k}_1, \dots, \bar{k}_n\}) \dots),$$

$$F = \int_{k_{min}}^{k_{max}} dk_{\gamma} d \cos \theta_{\gamma} d\phi_{\gamma} f(k_{\gamma}, \theta_{\gamma}, \phi_{\gamma}). \leftarrow \text{KLN good start}$$

- The **olive** parts of rhs. give crude distribution over tangent space, The whole formula is of the lowest order in exponentiation scheme **Eikonal level only!**

WE define the complete set of spin amplitudes for emission of  $n$  photons in  $\mathcal{O}(\alpha^r)_{\text{CEEX}}$ ,  $r = 0, 1, 2$  as follows:

$$\begin{aligned} \mathfrak{M}_n^{(0)} \left( \begin{matrix} p & k_1 & \dots & k_n \\ \lambda & \sigma_1 & \dots & \sigma_n \end{matrix} \right) &= \sum_{\{\varphi\}} \prod_{i=1}^n \mathfrak{s}_{[i]}^{\{\varphi_i\}} \beta_0^{(0)} \left( \begin{matrix} p \\ \lambda \end{matrix}; X_\varphi \right), \\ \mathfrak{M}_n^{(1)} \left( \begin{matrix} p & k_1 & \dots & k_n \\ \lambda & \sigma_1 & \dots & \sigma_n \end{matrix} \right) &= \sum_{\{\varphi\}} \prod_{i=1}^n \mathfrak{s}_{[i]}^{\{\varphi_i\}} \left\{ \beta_0^{(1)} \left( \begin{matrix} p \\ \lambda \end{matrix}; X_\varphi \right) + \sum_{j=1}^n \frac{\beta_{1\{\varphi_j\}}^{(1)} \left( \begin{matrix} p & k_j \\ \lambda & \sigma_j \end{matrix}; X_\varphi \right)}{\mathfrak{s}_{[j]}^{\{\varphi_j\}}} \right\}, \\ \mathfrak{M}_n^{(2)} \left( \begin{matrix} p & k_1 & \dots & k_n \\ \lambda & \sigma_1 & \dots & \sigma_n \end{matrix} \right) &= \\ &= \sum_{\{\varphi\}} \prod_{i=1}^n \mathfrak{s}_{[i]}^{\{\varphi_i\}} \left\{ \beta_0^{(2)} \left( \begin{matrix} p \\ \lambda \end{matrix}; X_\varphi \right) + \sum_{j=1}^n \frac{\beta_{1\{\varphi_j\}}^{(2)} \left( \begin{matrix} p & k_j \\ \lambda & \sigma_j \end{matrix}; X_\varphi \right)}{\mathfrak{s}_{[j]}^{\{\varphi_j\}}} + \sum_{1 \leq j < l \leq n} \frac{\beta_{2\{\varphi_j \varphi_l\}}^{(2)} \left( \begin{matrix} p & k_j & k_l \\ \lambda & \sigma_j & \sigma_l \end{matrix}; X_\varphi \right)}{\mathfrak{s}_{[j]}^{\{\varphi_j\}} \mathfrak{s}_{[l]}^{\{\varphi_l\}}} \right\}. \end{aligned}$$

The *coherent* sum is taken over set  $\{\varphi\}$  of all  $2^n$  partitions – the partition  $\varphi$  is defined as a vector  $(\varphi_1, \varphi_2, \dots, \varphi_n)$ ;  $\varphi_i = 1$  for an ISR and  $\varphi_i = 0$  for an FSR photon. The set of all partitions is explicitly the following:

$$\{\varphi\} = \{(0, 0, 0, \dots, 0), (1, 0, 0, \dots, 0), (0, 1, 0, \dots, 0), (1, 1, 0, \dots, 0), \dots (1, 1, 1, \dots, 1)\}.$$

The  $s$ -channel four-momentum in the (possibly) resonant  $s$ -channel propagator is

$$X_\varphi = p_a + p_b - \sum_{i=1}^n \varphi_i k_i.$$

At  $\mathcal{O}(\alpha^r)$  we have to provide functions  $\beta_k^{(r)}$ ,  $k = 0, 1, \dots, r$ , from Feynman diagrams, which are infrared-finite by construction [yfs:1961](#). Their actual precise definitions can be found in other refs. on KKMC. Here we shall define only

the most essential ingredients. The lowest-order  $\beta_0^{(0)}$  are just Born spin amplitudes times a certain kinematical factor

$$\beta_0^{(0)}(p_\lambda; X) = \mathfrak{B}(p_\lambda; X) \frac{X^2}{(p_c + p_d)^2}. \quad (19)$$

The Born spin amplitudes  $\mathfrak{B}(p_\lambda; X)$  and other spin amplitudes are calculated using the spinor technique of Kleiss and Stirling (KS) reformulated a bit.. Soft factors  $\mathfrak{s}_{[i]}^{(\omega)}$ ,  $\omega = 0, 1$ , are complex numbers, see ref. for exact definitions; here we only need to know their absolute values

$$\left| \mathfrak{s}_{[i]}^{(1)} \right|^2 = -\frac{e^2 Q_e^2}{2} \left( \frac{p_a}{k_i p_a} - \frac{p_b}{k_i p_b} \right)^2, \quad \left| \mathfrak{s}_{[i]}^{(0)} \right|^2 = -\frac{e^2 Q_f^2}{2} \left( \frac{p_c}{k_i p_c} - \frac{p_d}{k_i p_d} \right)^2. \quad (20)$$

The factor  $\bar{\Theta}(\Omega)$  defines the infrared (IR) integration limits for real photons. More precisely for a single photon, complementary domain  $\Omega$  includes the IR divergence point  $k = 0$ , which is *excluded* from the MC phase space, we define a characteristic function  $\Theta(\Omega, k) = 1$  for  $k \in \Omega$  and  $\Theta(\Omega, k) = 0$  for  $k \notin \Omega$ . The characteristic function for the phase space included in the integration is  $\bar{\Theta}(\Omega, k) = 1 - \Theta(\Omega, k)$ . The characteristic function for *all* photons in the MC phase space is

$$\bar{\Theta}(\Omega) = \prod_{i=1}^n \bar{\Theta}(\Omega, k_i). \quad (21)$$

In the present program we opt for an  $\Omega$  traditionally defined by the photon energy cut condition  $k^0 < E_{\min}$ .

Consequently, the YFS form factor reads

$$\begin{aligned}
 Y(\Omega; p_a, \dots, p_d) &= Q_e^2 Y_\Omega(p_a, p_b) + Q_f^2 Y_\Omega(p_c, p_d) \\
 &+ Q_e Q_f Y_\Omega(p_a, p_c) + Q_e Q_f Y_\Omega(p_b, p_d) - Q_e Q_f Y_\Omega(p_a, p_d) - Q_e Q_f Y_\Omega(p_b, p_c),
 \end{aligned}
 \tag{22}$$

where

$$\begin{aligned}
 Y_\Omega(p_1, p_2) &\equiv 2\alpha \tilde{B}(\Omega, p_1, p_2) + 2\alpha \Re B(p_1, p_2) \\
 &\equiv -2\alpha \frac{1}{8\pi^2} \int \frac{d^3 k}{k^0} \Theta(\Omega; k) \left( \frac{p_1}{kp_1} - \frac{p_2}{kp_2} \right)^2 \\
 &+ 2\alpha \Re \int \frac{d^4 k}{k^2} \frac{i}{(2\pi)^3} \left( \frac{2p_1 + k}{2kp_1 + k^2} - \frac{2p_2 - k}{2kp_2 - k^2} \right)^2
 \end{aligned}
 \tag{23}$$

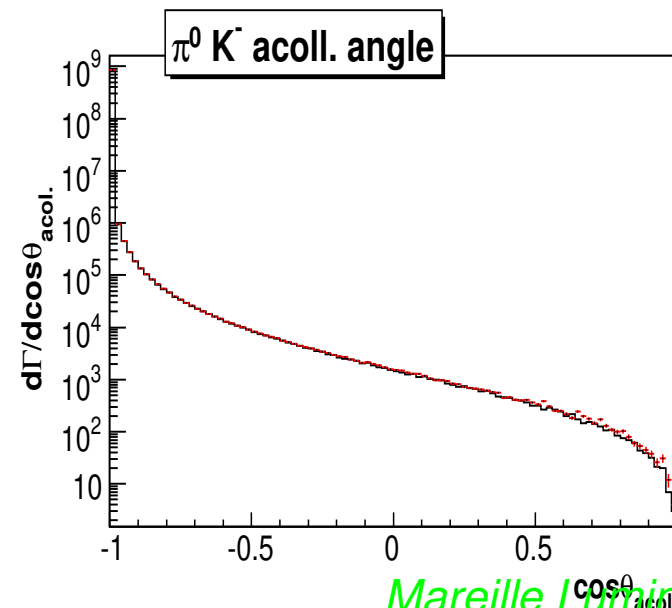
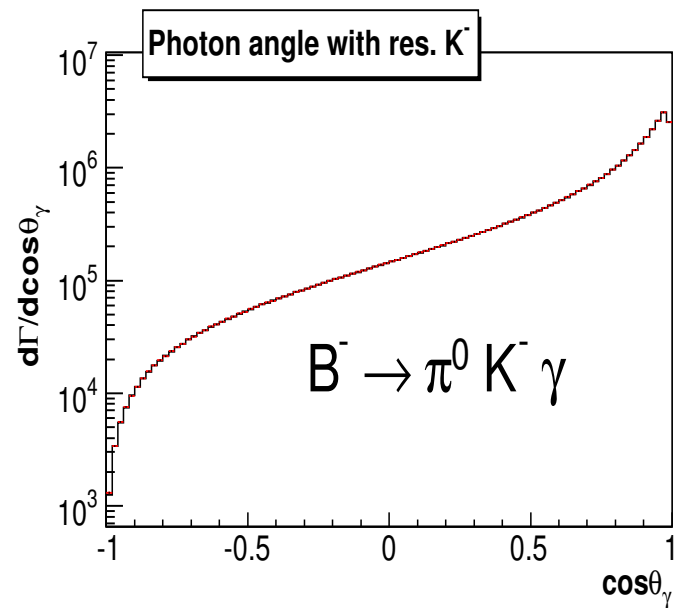
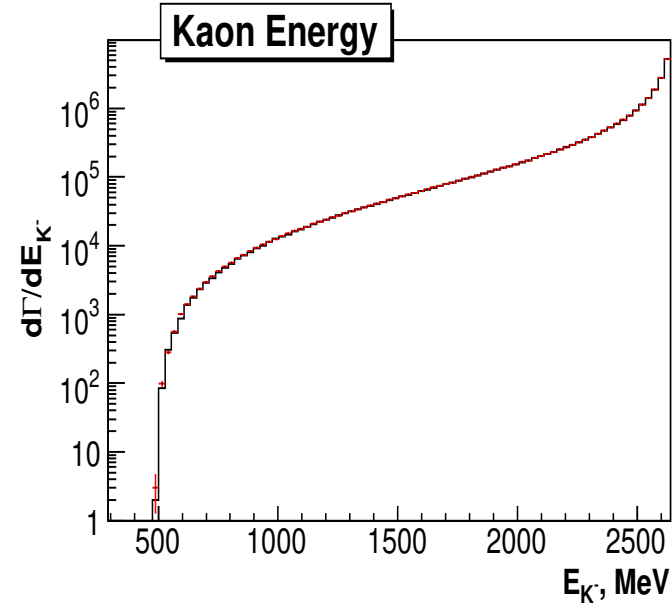
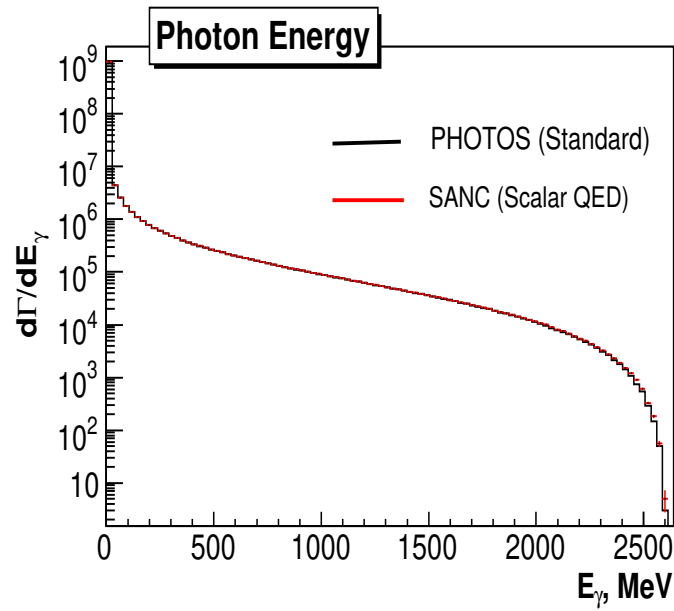


Basic formula is the same (OK it is similar only but differ in essential results)

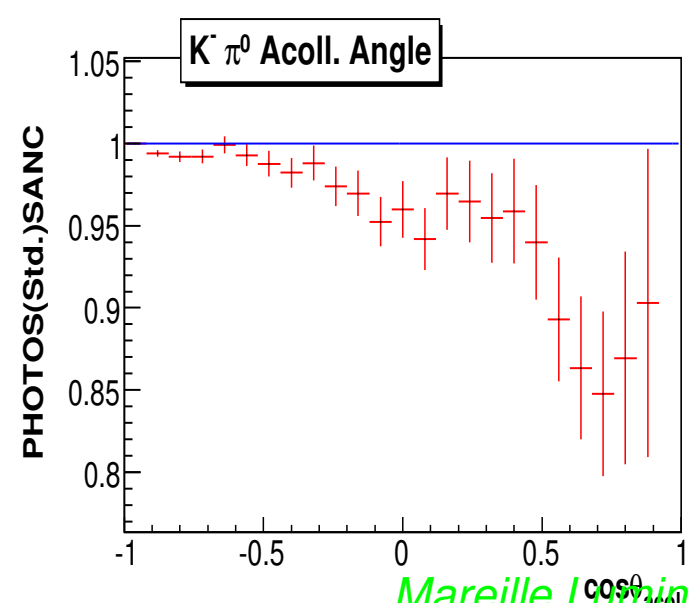
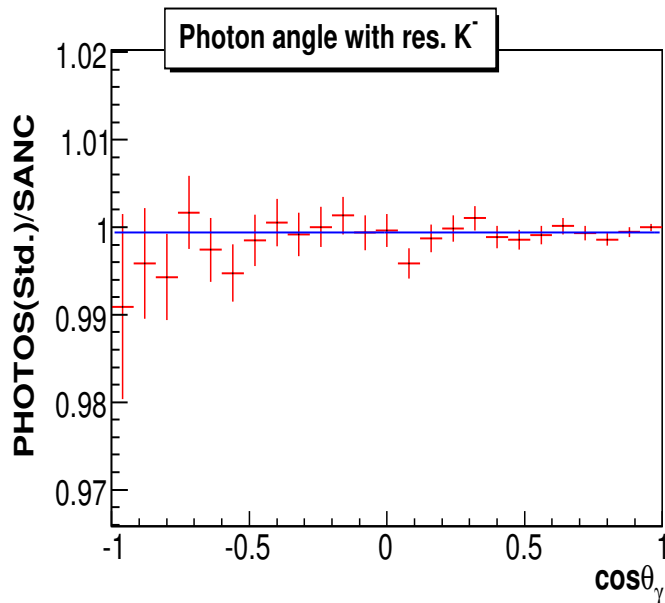
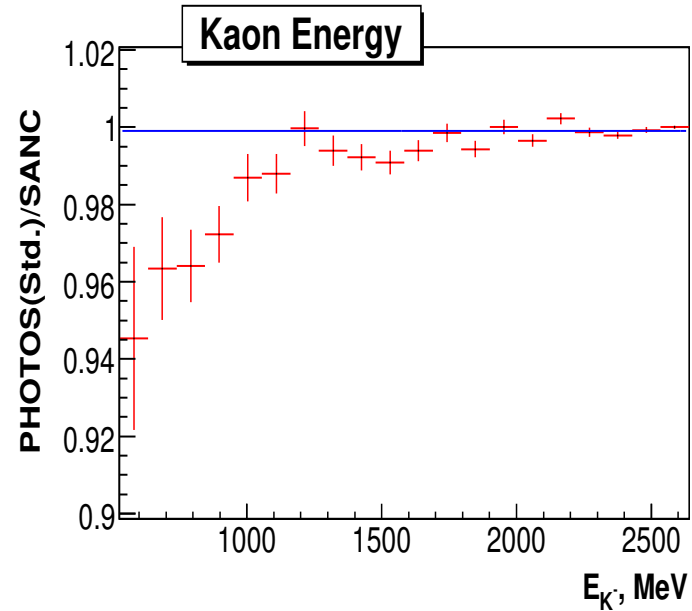
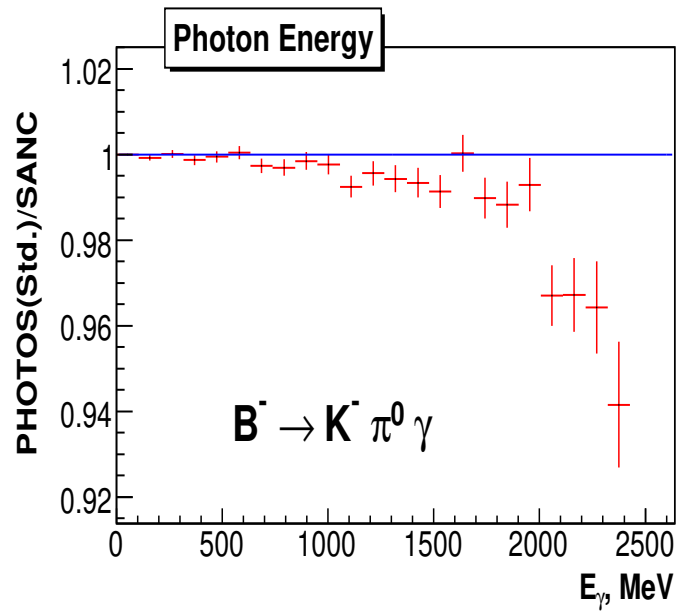
1. for phase space limits iterative solution instead of re-scaling available thanks to conformal symmetry is used.
2. Instead of expansion of matrix elements into  $\beta_i^{(1)}$  and sum over partition, products of  $(s_i + \beta_i^{(1)})$  of each photon is used.
3. surprisingly this does not destroy second order parts, but help include the dominant parts of that.
4.  $\beta_i^{(1)}$  as used in photos consist of process independent part, (after integration it gives LL parts), but also process dependent parts (for some decays only).
5. I should say more about virtual corrections.
6. for emission kernels they can be simply coded as form-factors.
7. Far more fundamental is what to do with loop corrections beyond KLM level. They need to be included in rates of events prior `photos`.
8. That is questionable statement already for two-body decays.

9. for more than two body substantial work may be needed for high precision level.

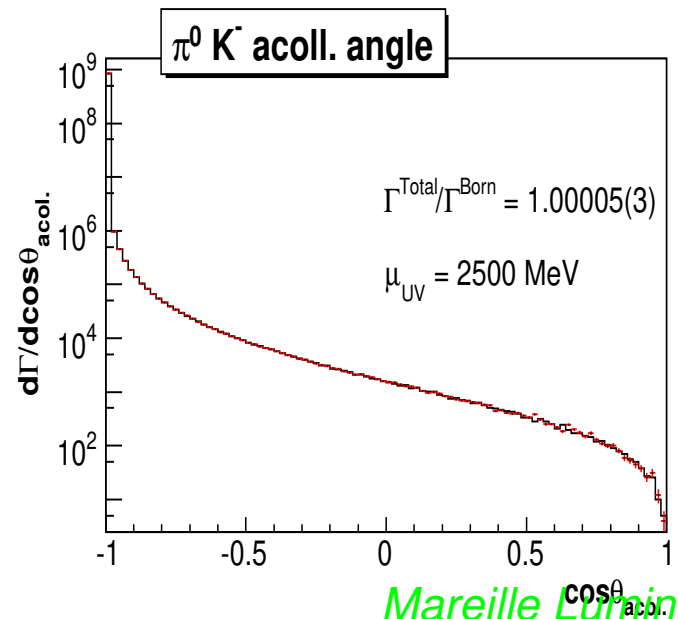
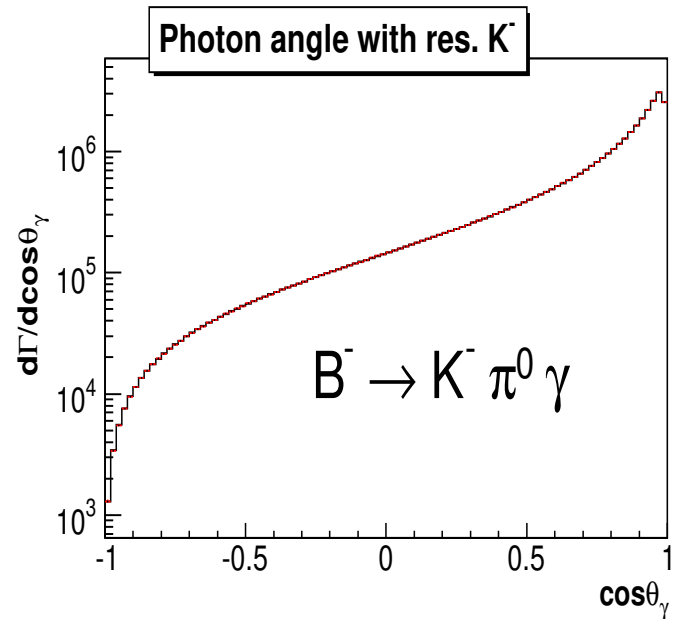
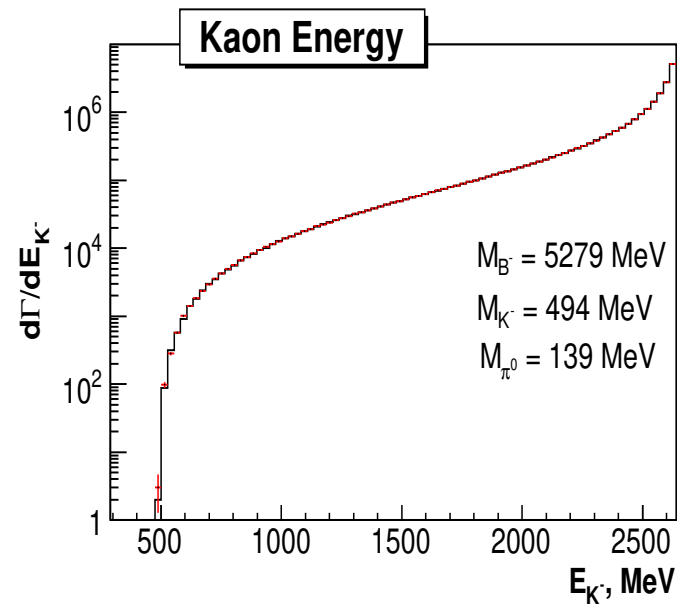
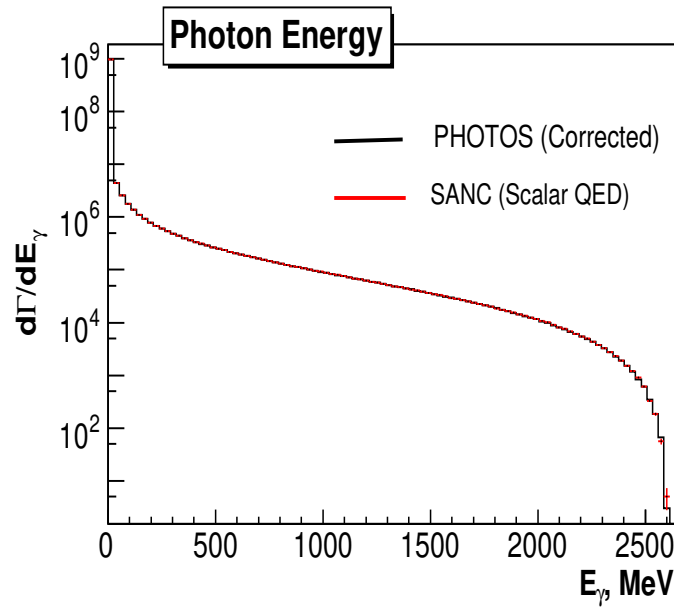
$B^- \rightarrow \pi^0 K^-$  : standard PHOTOS looks good. but ...



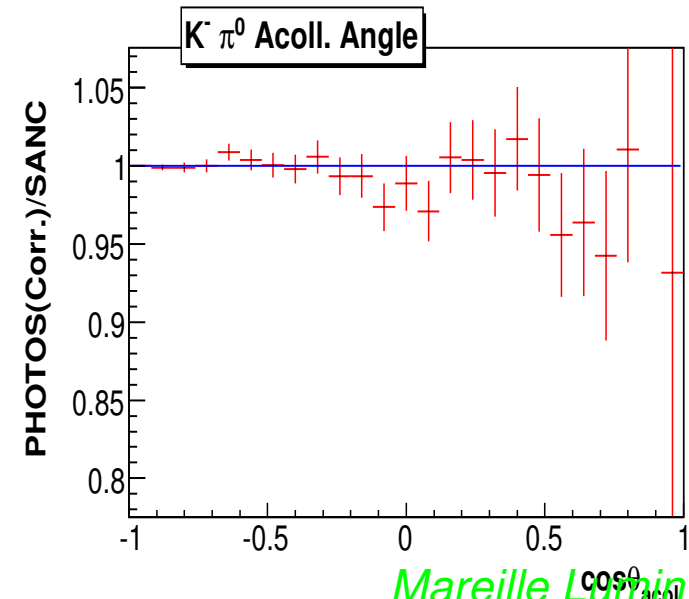
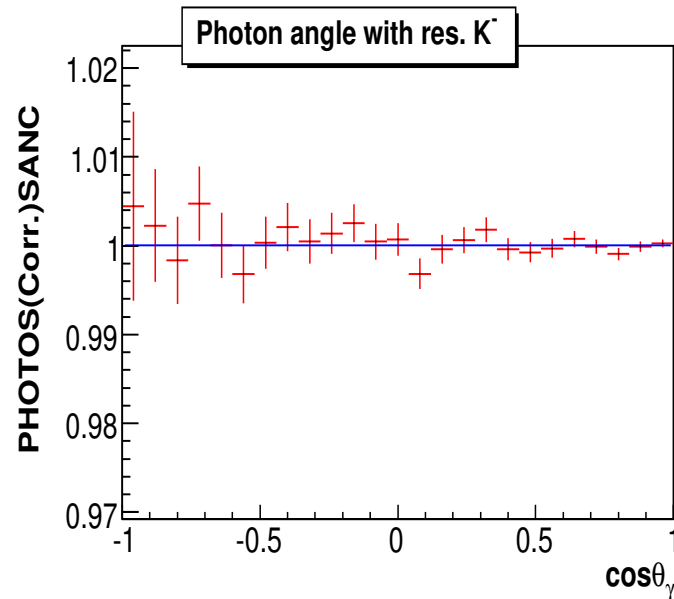
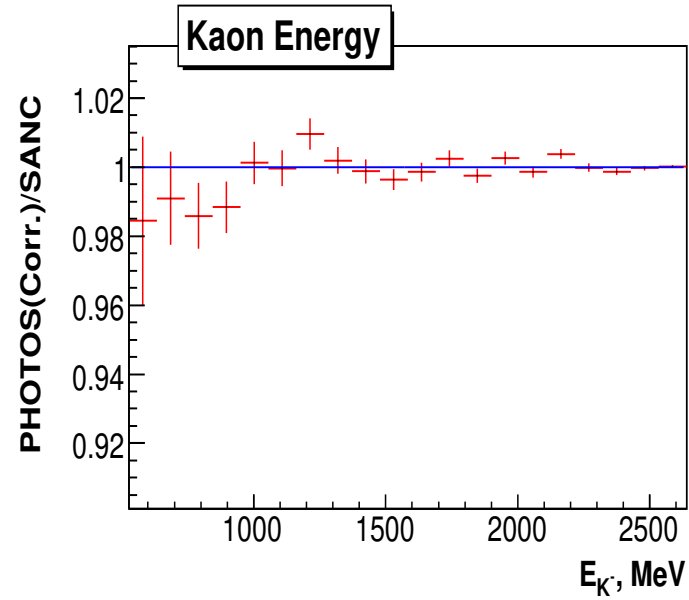
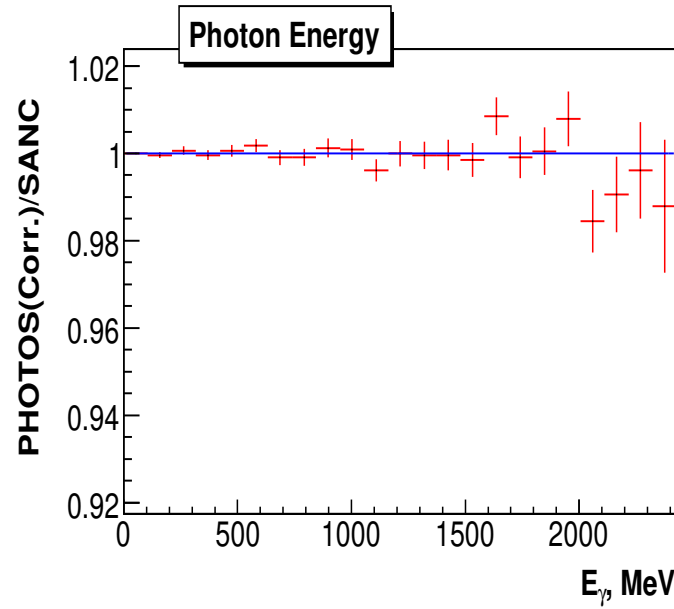
$B^- \rightarrow \pi^0 K^-$  · standard PHOTOS not perfect



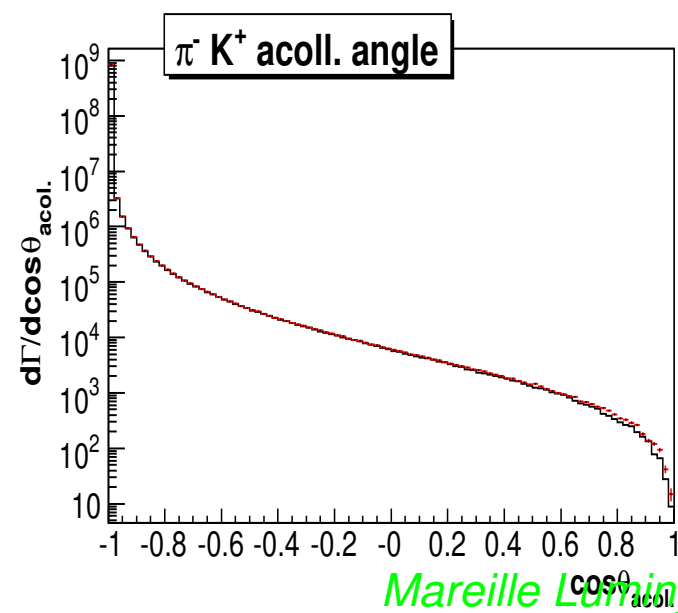
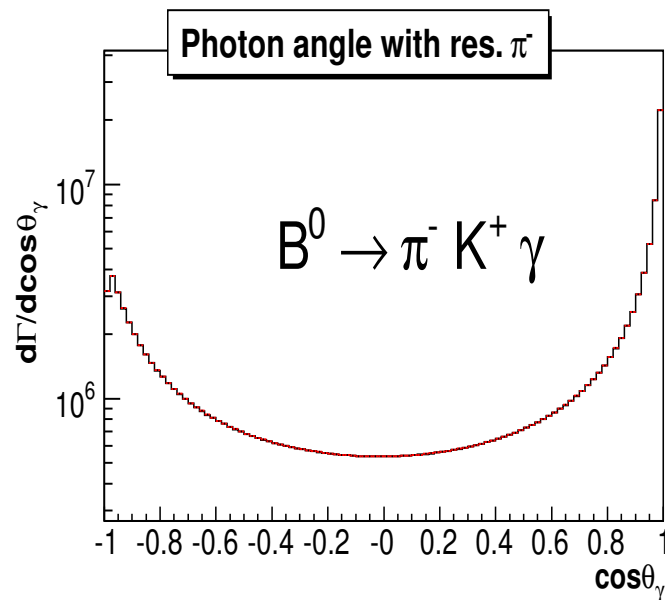
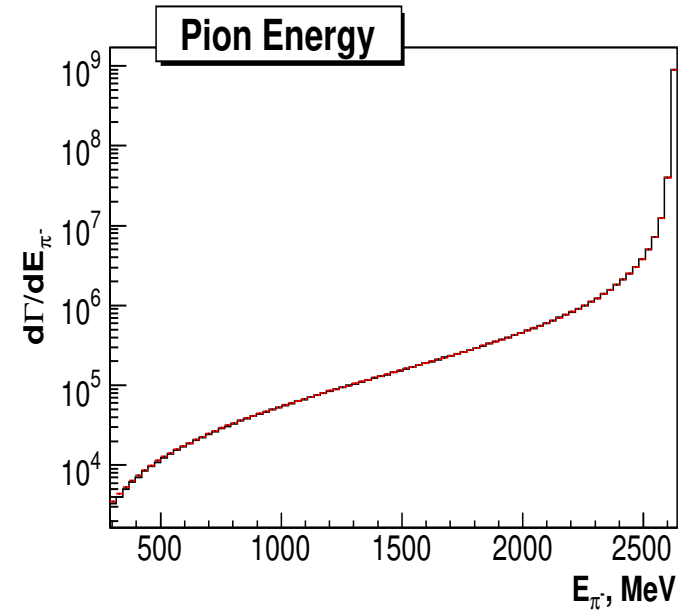
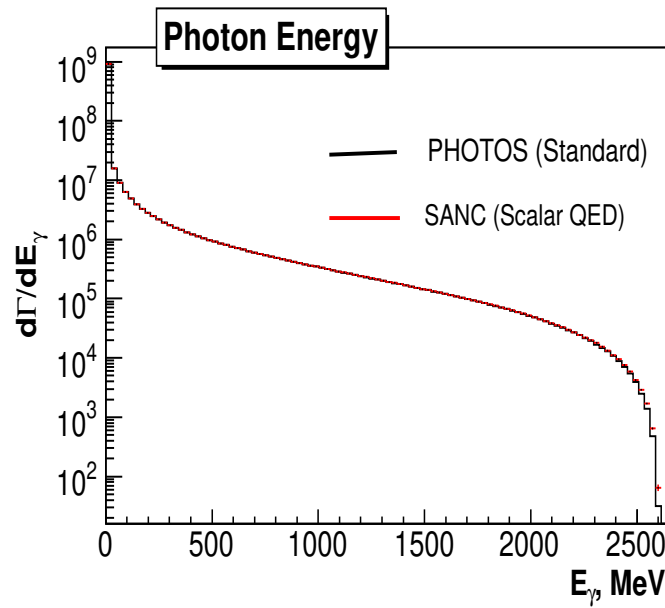
$B^- \rightarrow \pi^0 K^- \cdot MF$  improved PHOTOS Looks good



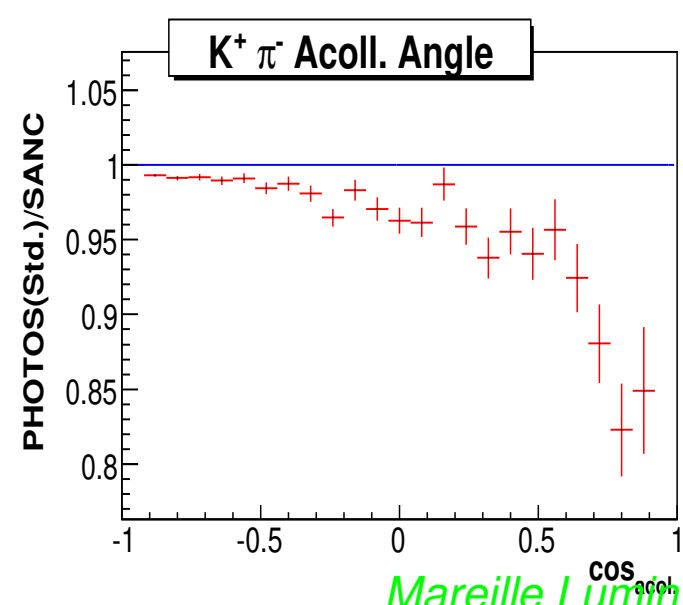
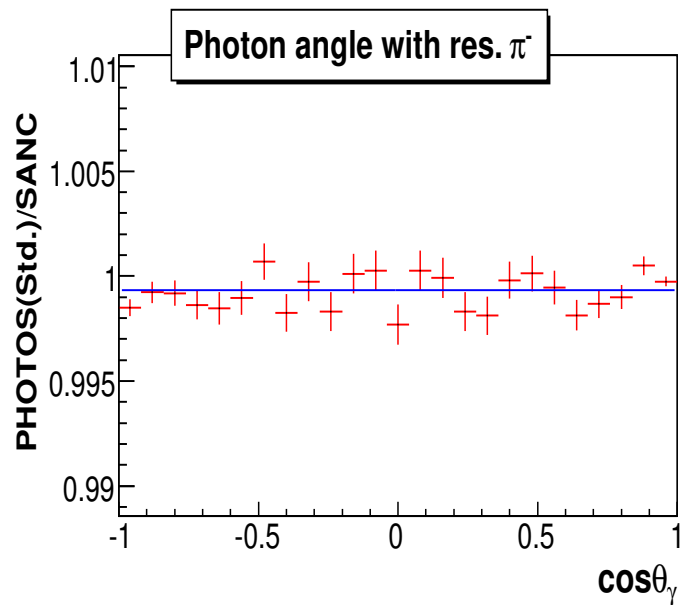
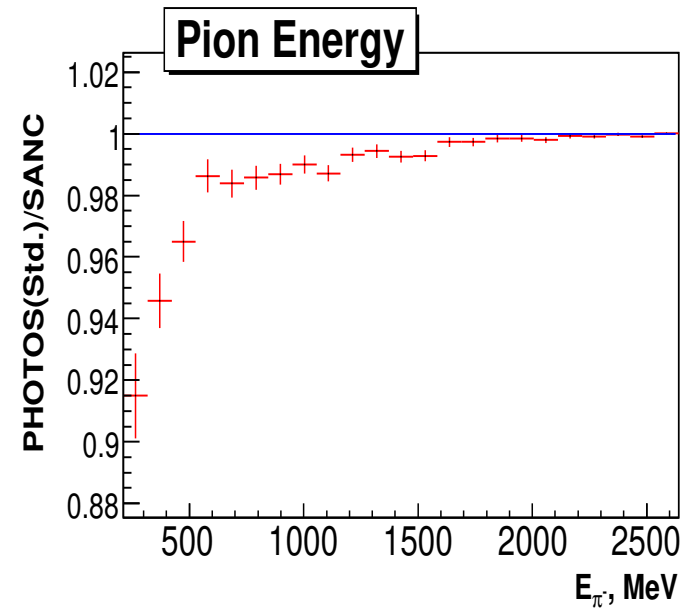
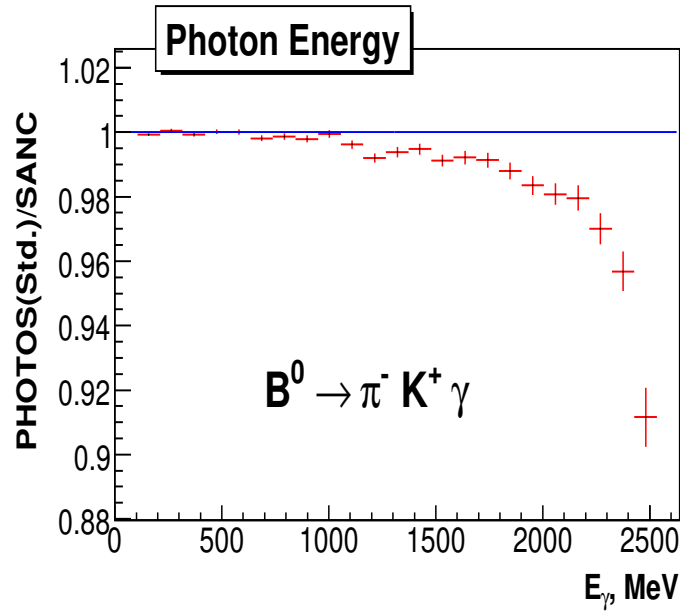
$B^- \rightarrow \pi^0 K^-$  : ME improved PHOTOS ... and is good.



$B^0 \rightarrow \pi^- K^+$ : standard PHOTOS Looks good ...

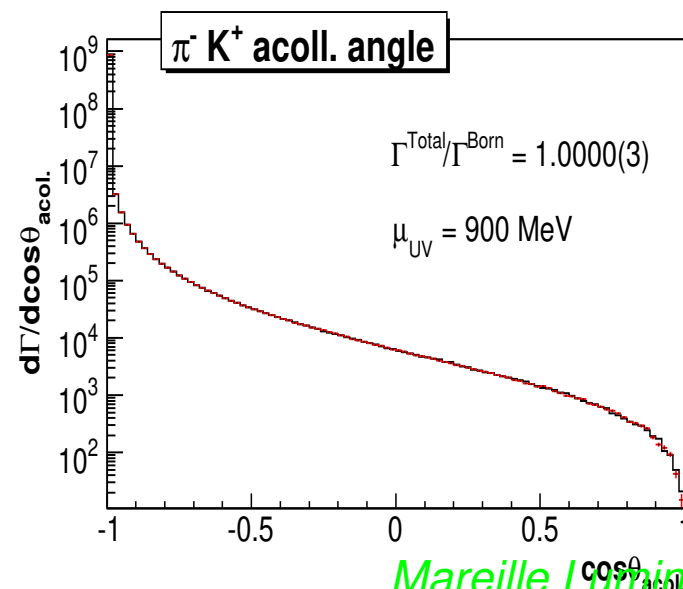
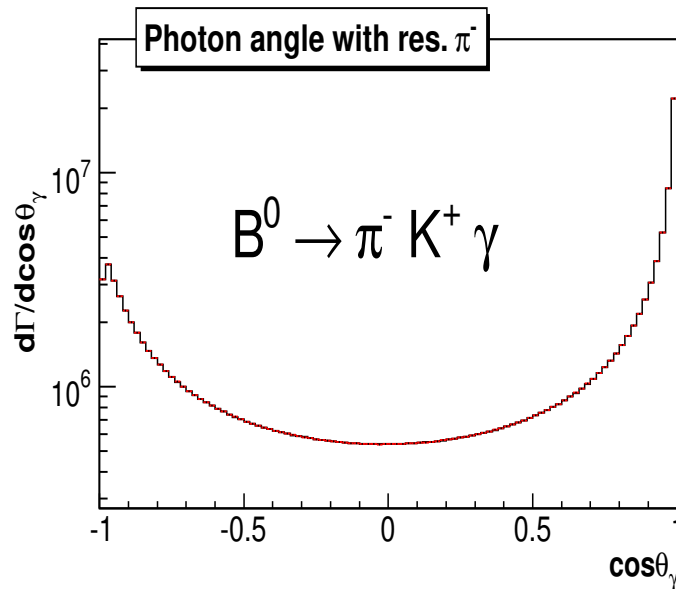
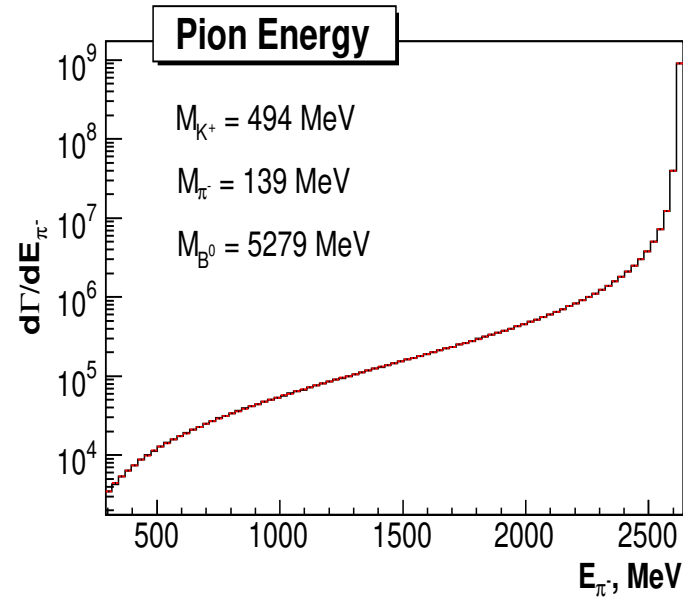
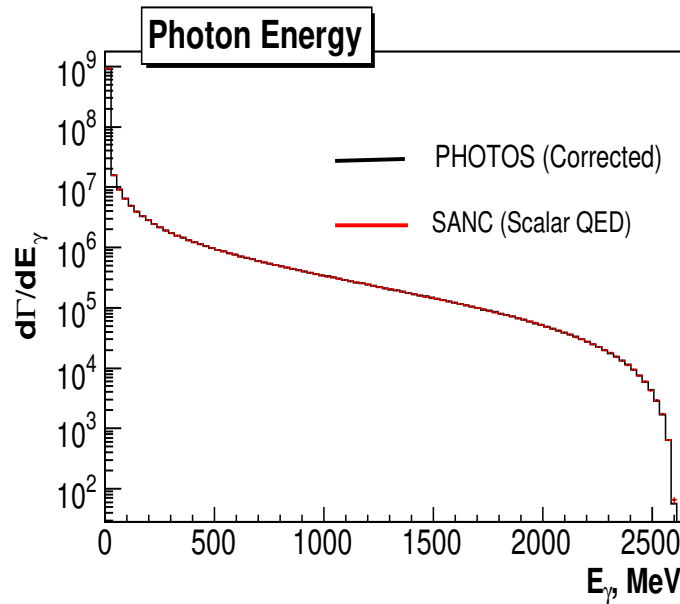


$B^0 \rightarrow \pi^- K^+ \gamma$ : standard PHOTOS ... but not perfect.

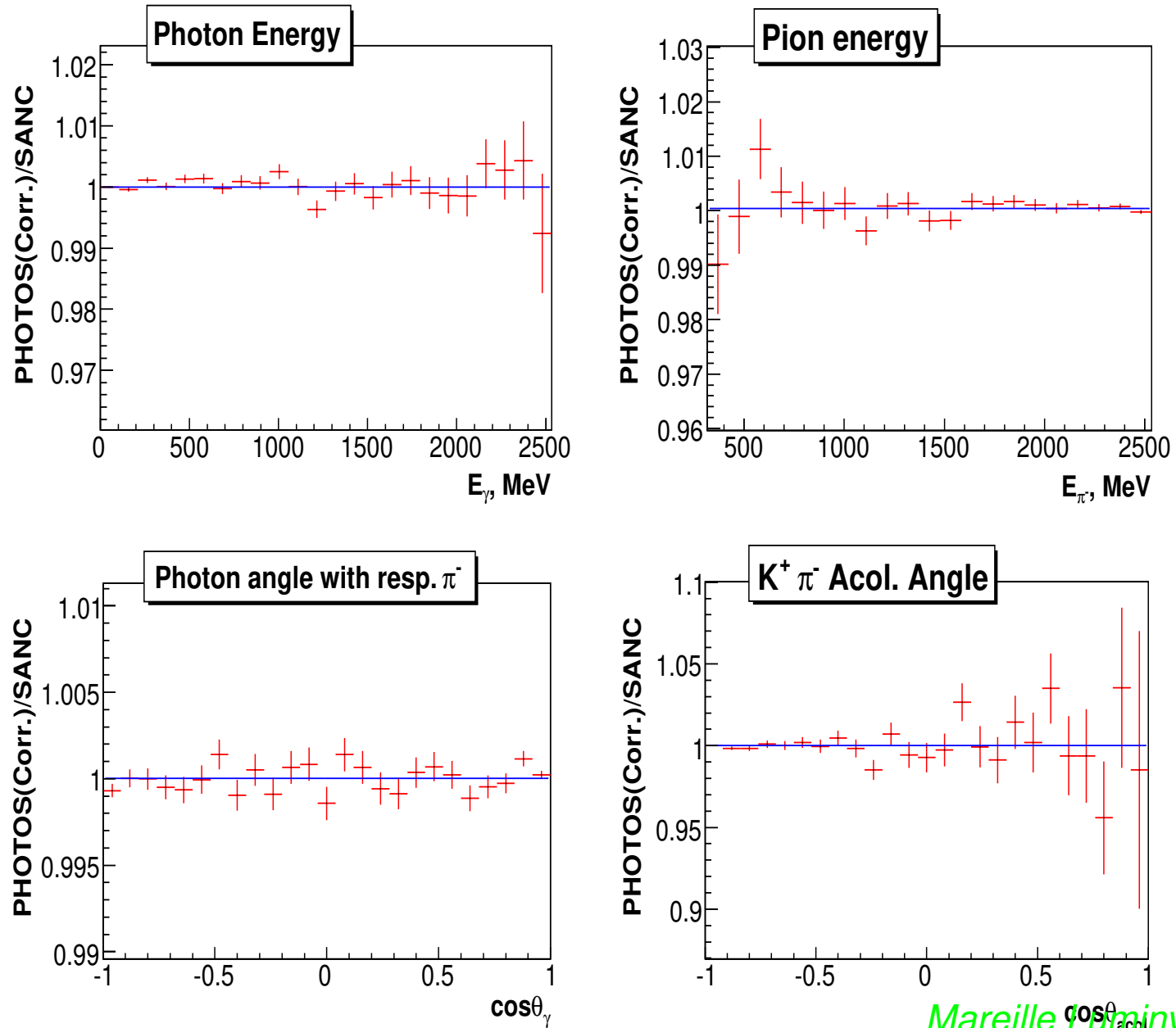




$B^0 \rightarrow \pi^- K^+ : ME \text{ improved PHOTOS}$  Looks good ...



$B^0 \rightarrow \pi^- K^+$ ; ME improved PHOTOS ... also perfect !



*Other processes*

Results for  $W$ ,  $H$ , and  $\gamma^* \rightarrow \pi^+ \pi^-$  are of similar quality.

**Important:** For  $\gamma^* \rightarrow \pi^+ \pi^-$  ME corrections were larger than in other cases

Tests for  $K^\pm \rightarrow l^\pm \nu \pi^+ \pi^-$  were started but fall from the table. In general for more than two body decays effort for tests/developments was never enough to match sophistication of the one presented earlier.

... but of importance.

## Essential details to preserve spin correlations

Note that the spin carried out by photon is in most cases zero, orbital and spin of photon cancel out completely in soft and collinear limit.

only in ultra-hard ultra collinear configurations of  $\sim 1/3\alpha/\pi$  weight it is not the case.

PHOTOS was developed keeping that in mind. **PURPOSE:** not to destroy spin correlations of the consecutive decays.

1. we are using **STANDARD and FORMAL** parametrizations of Lorentz group. One can express it with the help of consecutive boosts and rotations.
2. Convenient for Monte Carlo event construction!
3. For the definition of coordinate system in the  $P$ -rest frame the  $\hat{x}$  and  $\hat{y}$  axes of the laboratory frame boosted to the rest frame of  $P$  can be used. The orthogonal right-handed system can be constructed with their help in a standard way.
4. We choose polar angles  $\theta_1$  and  $\phi_1$  defining the orientation of the four momentum  $\bar{k}_2$  in the rest frame of  $P$ . In that frame  $\bar{k}_1$  and  $\bar{k}_2$  are back to back<sup>a</sup>, see fig. (1).
5. The previous two points would complete the definition of the two-body phase space, if both  $\bar{k}_1$  and  $\bar{k}_2$  had no measurable spin degrees of freedom visualizing themselves e.g. through correlations of the secondary decay products' momenta. Otherwise we need to know an additional angle  $\phi_X$  to complete the set of Euler angles defining the relative orientation of the axes of the  $P$  rest-frame system with the coordinate system used in the rest-frame of  $\bar{k}_2$  (and possibly also of  $\bar{k}_1$ ), see fig. (2).

---

<sup>a</sup>In the case of phase space construction for multi-body decays  $\bar{k}_2$  should read as a state representing the sum of all decay products of  $P$  but  $\bar{k}_1$ .

6. If both rest-frames of  $\bar{k}_1$  and  $\bar{k}_2$  are of interest, their coordinate systems are oriented with respect to  $P$  with the help of  $\theta_1, \phi_1, \phi_X$ . We assume that the coordinate systems of  $\bar{k}_1$  and  $\bar{k}_2$  are connected by a boost along the  $\bar{k}_2$  direction, and in fact share axes:  $z' \uparrow\downarrow z'', x' \uparrow\uparrow x'', y' \uparrow\downarrow y''$ .
7. For the three-body phase space: We take the photon energy  $k_\gamma$  in  $P$  rest frame. We calculate: photon,  $k_1$  and  $k_2$  energies, all in  $k_1 + k_2$  frame.
8. We use the angles  $\theta, \phi$ , in the rest-frame of the  $k_1 + k_2$  pair: angle  $\theta$  is an angle between the photon and  $k_1$  direction (i.e.  $-z''$ ). Angle  $\phi$  defines the photon azimuthal angle around  $z''$ , with respect to  $x''$  axis (of the  $k_2$  rest-frame), see fig. (3).
9. If all  $k_1, k_2$  and  $k_1 + k_2$  rest-frames exist, then the  $x$ -axes for the three frames are chosen to coincide. It is OK, all frames connected by boosts along  $z''$  see fig. (3).
10. To define orientation of  $k_2$  in  $P$  rest-frame coordinate system, and to complete construction of the whole event, we will re-use Euler angles of  $\bar{k}_2$ :  $\phi_X, \theta_1$  and  $\phi_1$  (see figs. 4 and 5), defined again of course in the rest frame of  $P$ .

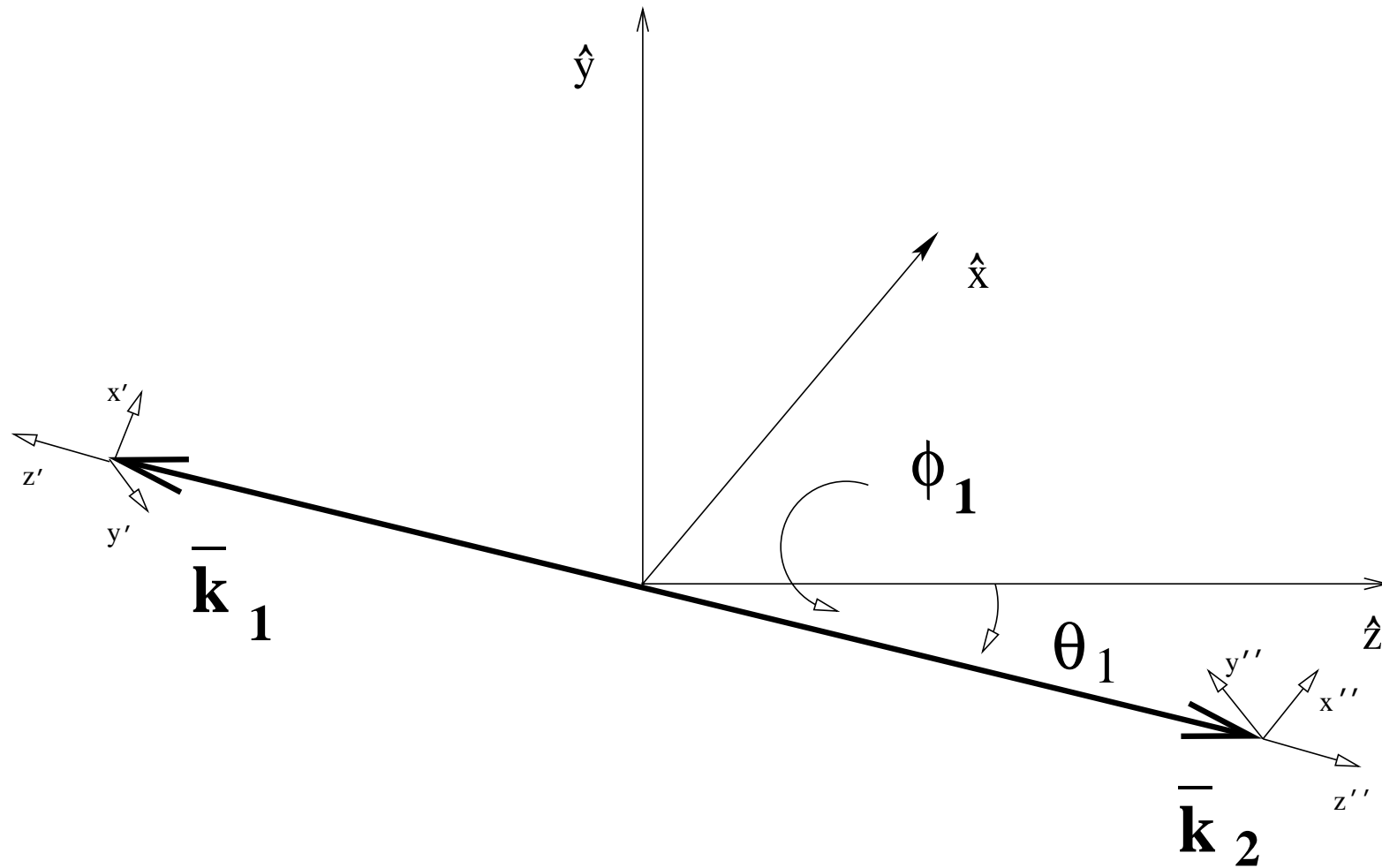


Figure 1: The angles  $\theta_1$ ,  $\phi_1$  defined in the rest-frame of  $P$  and used in parametrization of two-body phase-space.

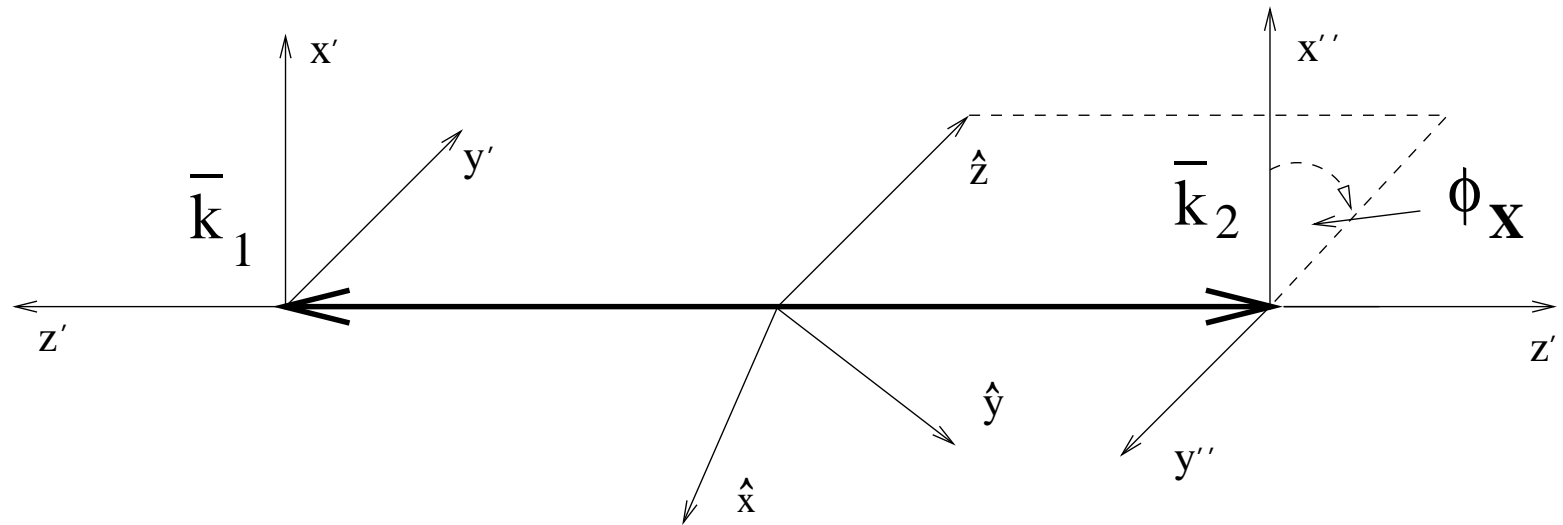


Figure 2: Angle  $\phi_X$  is also defined in the rest-frame of  $P$  as an angle between (oriented) planes spanned on: (i)  $\bar{k}_1$  and  $\hat{z}$ -axis of the  $P$  rest-frame system, and (ii)  $\bar{k}_1$  and  $x''$ -axis of the  $\bar{k}_2$  rest frame. It completes definition of the phase-space variables if internal orientation of  $\bar{k}_1$  system is of interest. In fact, Euler angle  $\phi_X$  is inherited from unspecified in details, parametrization of phase space used to describe possible future decay of  $\bar{k}_2$  (or  $\bar{k}_1$ ).



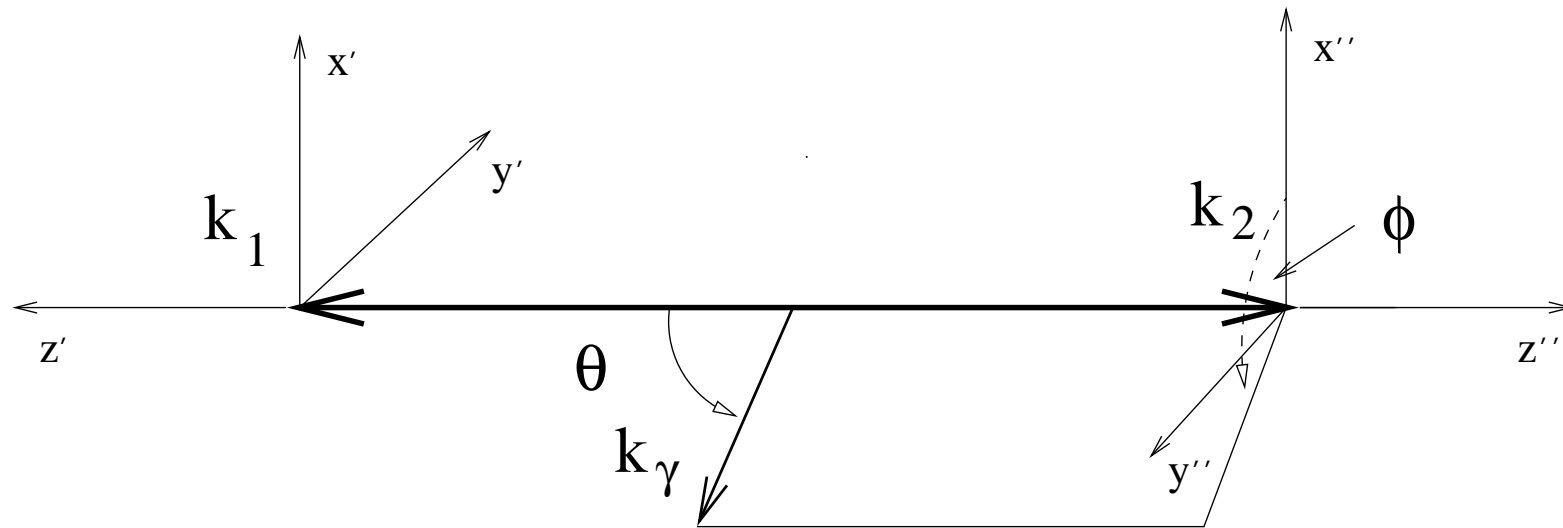


Figure 3: The angles  $\theta$ ,  $\phi$  are used to construct the four-momentum of  $k_\gamma$  in the rest-frame of  $k_1 + k_2$  pair (itself not yet oriented with respect to  $P$  rest-frame). To calculate energies of  $k_1$ ,  $k_2$  and photon, it is enough to know  $m_1$ ,  $m_2$ ,  $M$  and photon energy  $k_\gamma$  of the  $P$  rest-frame.

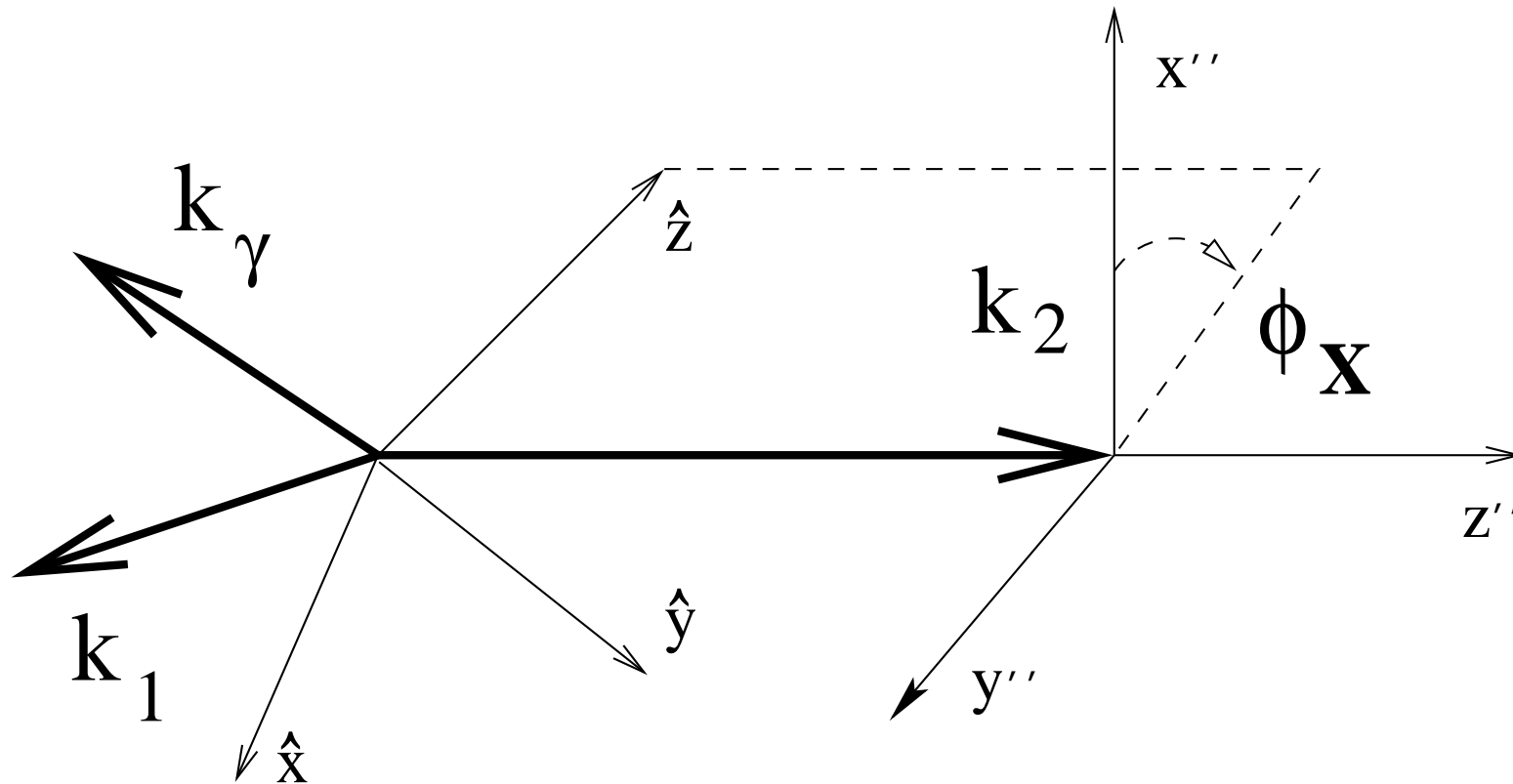


Figure 4: Use of angle  $\phi_x$  in defining orientation of  $k_1$ ,  $k_2$  and photon in the rest-frame of  $P$ . At this step only the plane spanned on  $P$  frame axis  $\hat{z}$  and  $k_2$  is oriented with respect to  $k_2 \times x''$  plane.

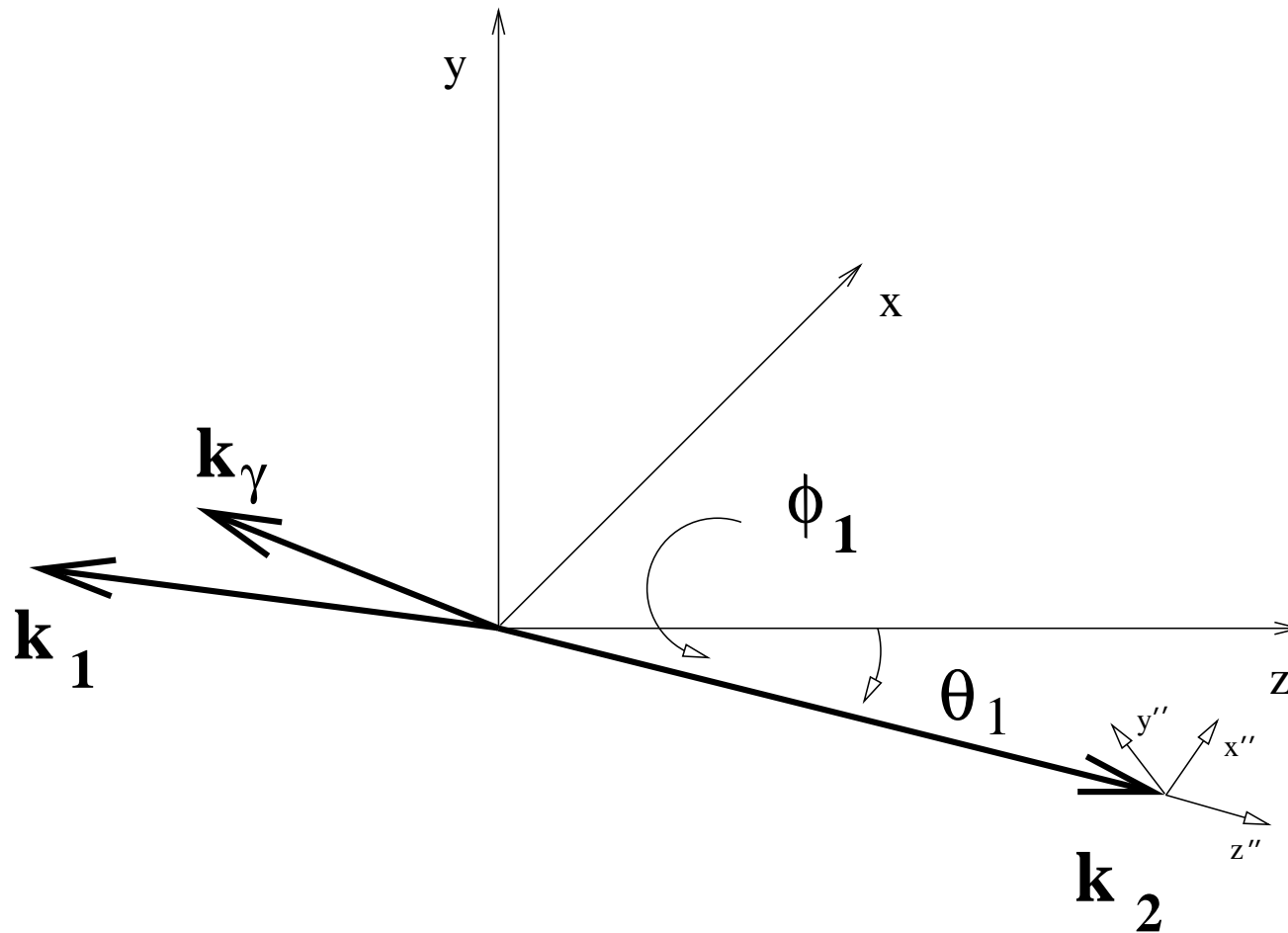


Figure 5: Final step in event construction. Angles  $\theta_1$ ,  $\phi_1$  are used. The final orientation of  $k_2$  coincide with this of  $\bar{k}_2$ .